NAVAL OCEAN SYSTEMS CENTER
San Diego, California 92152

28 January 1980

NOSC TR 652
FIBER-OPTIC COMMUNICATION LINKS FOR UNMANNED INSPECTION SUBMERSIBLES, by SJ Cowan, PJ Heckman, and M Kono, 15 October 1980

# LITERATURE CHANGE

Please make the following changes to your copy of NOSC TR 652.

On page 11, table 1, under PHYSICAL CHARACTERISTICS, the entries for Breadth and Height for the EAVE EAST vehicle should read 60 and 36, respectively.

UNCLASSIFIED

SECURITY CLASSIFICATION OF THIS PAGE *(When Data Entered)*

## REPORT DOCUMENTATION PAGE

READ INSTRUCTIONS BEFORE COMPLETING FORM

1. REPORT NUMBER: NOSC Technical Report 652 (TR 652)

2. GOVT ACCESSION NO.:

3. RECIPIENT'S CATALOG NUMBER:

4. TITLE *(and Subtitle)*: FIBER-OPTIC COMMUNICATION LINKS FOR UNMANNED INSPECTION SUBMERSIBLES

5. TYPE OF REPORT & PERIOD COVERED:

6. PERFORMING ORG. REPORT NUMBER:

7. AUTHOR(s):
S.J. Cowan
P.J. Heckman
Michael Kono

8. CONTRACT OR GRANT NUMBER(s):

9. PERFORMING ORGANIZATION NAME AND ADDRESS:
Naval Ocean Systems Center
San Diego, CA 921152

10. PROGRAM ELEMENT, PROJECT, TASK AREA & WORK UNIT NUMBERS:
FGOV, 521-MS31

11. CONTROLLING OFFICE NAME AND ADDRESS:
U.S. Geological Survey
620 National Center
Reston, VA 22092

12. REPORT DATE:
15 October 1980

13. NUMBER OF PAGES:
56

14. MONITORING AGENCY NAME & ADDRESS*(if different from Controlling Office)*:

15. SECURITY CLASS. *(of this report)*:
Unclassified

15a. DECLASSIFICATION/ DOWNGRADING SCHEDULE:

16. DISTRIBUTION STATEMENT *(of this Report)*:
Approved for public release; distribution unlimited

17. DISTRIBUTION STATEMENT *(of the abstract entered in Block 20, if different from Report)*:

18. SUPPLEMENTARY NOTES:

19. KEY WORDS *(Continue on reverse side if necessary and identify by block number)*:
Fiber optics
Unmanned submersibles
EAVE WEST
Communications
Underwater inspection
Offshore rigs
Underwater pipelines

20. ABSTRACT *(Continue on reverse side if necessary and identify by block number)*:

Periodic inspection of undersea pipelines and offshore structures requires depth capabilities in excess of those which are economical with divers (ie, 100 meters). Free-swimming, unmanned undersea vehicles operating in the supervisory-controlled mode (ie, man-in-the-loop) are being considered as a possible solution to the deep, undersea inspection problem. Specifically, an expendable optical fiber data link is proposed as a means to provide the wide-bandwidth, high-quality, bidirectional communications essential to advanced-sensor/real-time man-in-the-loop capabilities of such inspection vehicles.

DD FORM 1 JAN 73 1473 EDITION OF 1 NOV 65 IS OBSOLETE

S/N 0102-LF-014-6601

UNCLASSIFIED

SECURITY CLASSIFICATION OF THIS PAGE *(When Data Entered)*

## CONTENTS

## ILLUSTRATIONS



## TABLES

# 1.0 INTRODUCTION

Intimate relationships exist among the components of any undersea search, inspection, or work system. In general, such a system consists of a vehicle which performs the intended mission (ie, sensor suit, manipulators, etc), a support platform which provides all other required functions (power generation, data interpretation, command/control, etc), and a cable interfacing the above. A complex relationship exists between the functions of the vehicle, platform, and cable in that the respective requirements of these components are highly interactive. For example, the thrust of a tethered vehicle is proportional to the quantity of electrical power shipped to the vehicle but the cable diameter (hence the viscous drag force) is often proportional to the power transfer capability of the cable and thus necessitates greater thrust to propel the vehicle. This type of "vicious circle" can cause undersea systems to take on larger-than-expected physical dimensions and/or degrade considerably their intended performance expectations. For example, with traditional technologies, several tons of vehicle, cable, and deck and cable-handling systems may be required to transport a television camera weighing only a few pounds into the deep ocean environment for a simple inspection operation. Such an approach obviously carries with it inherent cost and logistical disadvantages.

## 1.1 UNDERSEA PIPELINES AND STRUCTURES INSPECTION

During the last decade, a vast amount of undersea drilling has taken place to tap our nation's oil and natural-gas reserves. More than 3000 structures were erected in the Gulf of Mexico alone within the last 10 years (ref 1). The eventual requirement for underwater inspection of these and the many more planned in the near future, together with their associated pipelines, is a growing concern. The cost of inspection is high now and is expected to get higher as drilling platforms move into deeper and more hazardous waters and as the complexity of the structures increases.

At present, the diver is the primary means of inspection in the offshore community. His principal tools have been visual inspection, photographs, and TV documentation. Manned submersibles have come into play and more recently tethered, unmanned submersibles have been used. However, there is a growing concern with problems of entanglement and ship support costs with these platforms. The availability of relatively inexpensive free-swimming (tetherless) robot vehicles may make routine underwater inspections and surveys for a vast number of pipelines and structures both economically feasible and practical but, without a communications link to the support platform, such a free-swimming system might be greatly hampered in capability in the near term. It is believed that the advantage of deployed fiber-optic communication links may hasten the practicality of such submersibles for two major reasons. First, the large bandwidth available with such a link allows the use of the same sensor systems and control-system technology currently used in tethered submersibles employed in such inspection missions but which require a much-larger-diameter cable. Secondly, the use of an inexpensive, deployed fiber-optic link promises to provide the same high-speed, entanglement-free operation as would be possible with an entirely autonomous vehicle.

## 1.2 GENERIC TYPES OF UNDERSEA VEHICLES

Figure 1 depicts several generic types of undersea vehicles. The most basic, the towed vehicle (fig 1A), consists of a towed sensor platform. The cable serves to impart

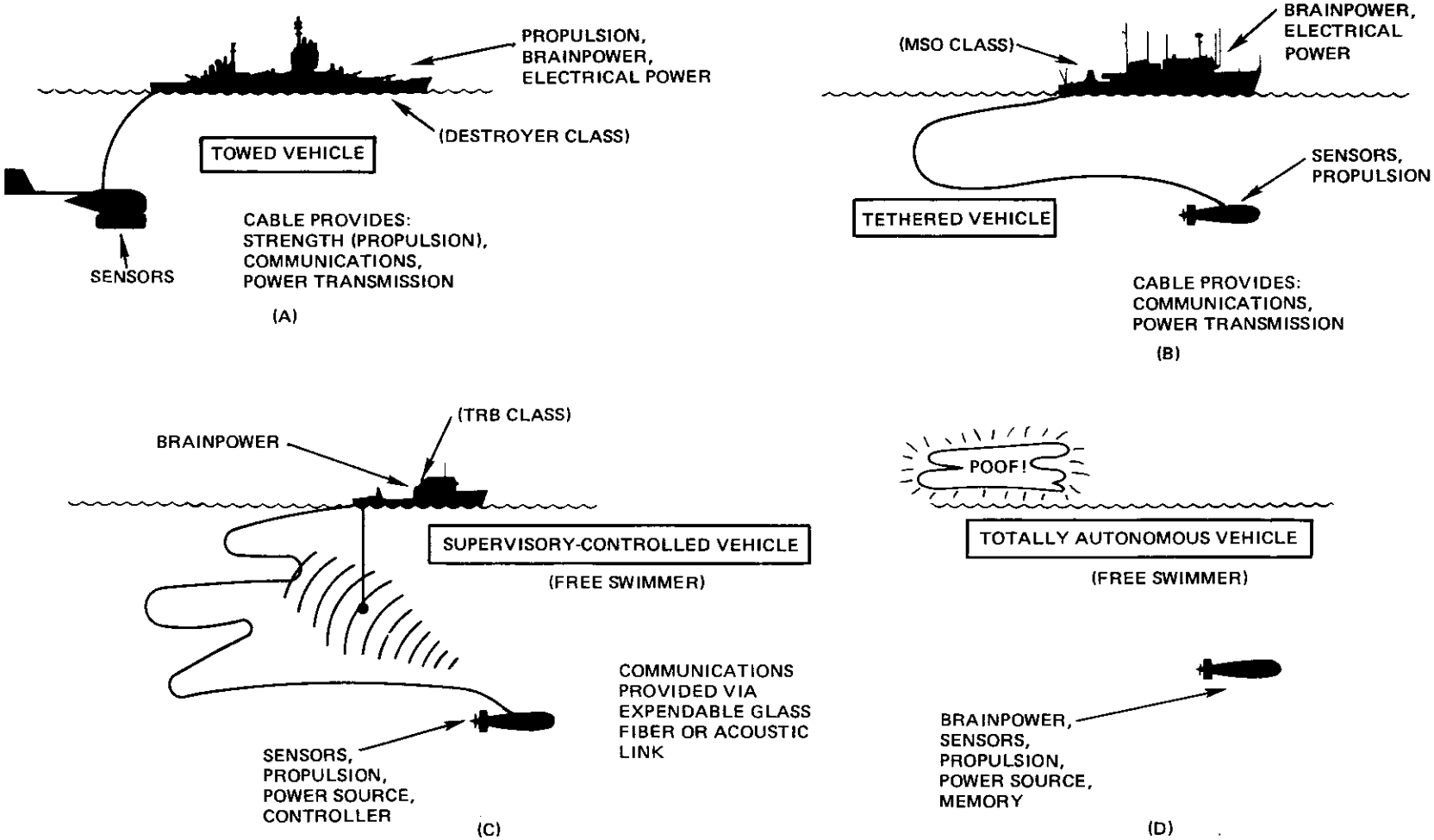


MORAL: AS MORE FUNCTIONS ARE TRANSFERRED FROM THE SURFACE CRAFT TO THE VEHICLE, REQUIREMENTS IMPOSED UPON THE SUPPORT CABLE AND SURFACE VESSEL ARE RELAXED (OR ELIMINATED!).

Figure 1. Classification of undersea, unmanned vehicle systems.

propulsion (by means of mechanical strength), provide electrical power (via metallic conductors), and provide communications (via coaxial transmission lines). Decisions, data interpretations, and command control are accomplished aboard ship; the vehicle is positioned by maneuvering the surface vessel and towing the package into place. Advantages include sizable payload weight, high speed, and long endurance. Disadvantages are low maneuverability, lack of "stop-and-look" capability, the need for a sizable surface support vessel, large turnaround space and time requirements for deep tow depths, and restrictions on direction of tow because of winds and currents.

A second approach, the tethered vehicle (fig 1B), attempts to overcome some of the disadvantages inherent in the towed system. In the tethered vehicle, propulsion is added to the sensor package so that the strength of the cable no longer serves in that role. Onboard propulsion gives the vehicle "stop-and-look" capability, which makes it highly maneuverable and reduces the required size of the support ship. The most critical function of the cable is now the electrical power transfer required to supply power for the vehicle's thrusters and sensors. It is desirable that such tethered cables be neutrally buoyant; hence exotic cabling materials such as copperclad aluminum, aramid fiber, and thermoplastic rubber are preferred in such applications. The tethered vehicle, having the ability to stop and "station keep" in the water, has the important advantage of becoming a remote work platform with a high degree of maneuverability. The price paid for maneuverability, however, is a reduction in speed and a "temperamental" cable arrangement which may become entangled or broken. The support ship also must have good stationkeeping ability to stay within "watch circle" of the submerged vehicle. In addition, substantial deck handling systems are still required for vehicle and cable. Moreover, the stage is set for the "vicious circle" between cable diameter and system size; as the system is required to go deeper and move faster, the cable must become larger.

Suppose that a tethered vehicle could be constructed which would carry an onboard power source for propulsion. The only remaining function of the cable now would be communications to and from the support vessel, and therefore the tether cable itself could be quite small in diameter. Such an approach is depicted in figure 1C. We have chosen to call this realization a "supervisory-controlled" vehicle. An example of this approach is the wire-guided torpedo. Such a system does not require great size to operate at great depths because it does not drag its tether behind; the tether is paid off or deployed from small storage canisters aboard the vehicle and tends to be nearly motionless in the water column even if the vehicle moves with great speed. Note that, since such a deployed link is expendable, entanglement is not a problem.

Unfortunately, metallic wire guides are unsuitable for inspection missions that require such wide-bandwidth sensors as television and high-resolution sonar because of bandwidth limitations (a few kilohertz over kilometer lengths, at best), but this shortcoming is relatively easy to overcome by using the wide available bandwidth capability of optical fiber technology. In addition, the high in-water weight of a metallic wire guide results in an unavoidable vehicle weight change caused by deployment of the heavy cable during the mission. For example, a weight savings of 15 to 1 was calculated for a 0.035-inch-diameter tether cable. This implies a differential weight change of approximately 100 pounds when lengths of 10 kilometers are to be deployed. The nearly neutrally buoyant fiber-optic cable, on the other hand, causes a much smaller vehicle trim problem under the same deployment conditions. Moreover, three recent technology breakthroughs have occurred within the last 5 to 10 years

which tend to make the concept of the supervisory-controlled vehicle both feasible and exciting. These are

1. The advent of strong, low-loss glass fibers, which allow many megahertz of signal bandwidth over many kilometers of nonmetallic transmission line literally as thin as a human hair.
2. The development of high-energy lithium batteries capable of providing the power to propel torpedo-sized vehicles for many kilometers at respectable speeds.
3. The appearance of the integrated circuit microprocessor, a remotely programmable computer-on-a-chip capable of making relatively complex control and interfacing decisions in situ and of guiding the vehicle safely home in the event of tether breakage.

Of course, if wide-bandwidth data transfer is not required for a particular mission, the tether cable can be dispensed with entirely and an acoustic communication link can be substituted. Such a system is still supervisory-controlled because of its man-in-the-loop capability. It appears possible to provide acoustic command control, and in some situations it may be feasible to transmit some uplink data such as slow-scan television. While such communication is neither high-resolution nor real-time, some situations may benefit from such a cableless approach so that the degradation incurred is entirely acceptable (ref 2). However, even in these cases the deployable optical fiber link may be superior as the primary communications channel because of its great noise immunity and lack of fade, with the acoustic capability serving as a backup in the event of a tether breakage.

In the most extreme case, the communications link could be eliminated entirely. A vehicle with artificial intelligence and huge memory capacity, the totally autonomous robotic vehicle (fig 1D), can be postulated with no man in the loop (and, moreover, no need for a support platform on station!). Such a robotic vehicle could be dropped (by aircraft or ship) into an area to perform an inspection mission, and, after performing its task, be recovered. The totally autonomous vehicle is not just a "blue-sky" concept; rather, it is a logical extension of the supervisory-controlled vehicle, and clearly will be feasible once already foreseeable advances in the technology permit its realization. In practice, it is expected that the distinction between the two vehicle types will be less than well defined as developments continue. Both approaches can be lumped together under the generic category of "free swimmers" or "free-swimming vehicles."

This report concentrates on the feasibility of a supervisory-controlled free swimmer; specifically, a system that deploys an optical fiber tether for communications purposes, with a supervisor that resides on a surface support platform.

## 1.3 FREE-SWIMMING VEHICLE TESTBEDS

There are at least two possible testbeds currently suitable for use as supervisory-controlled inspection vehicles upon which we can demonstrate the use of fiber-optic tethers. These are the vehicles which constitute the platform technology portion of the total U.S. Geological Survey Free-Swimming Submersible Technology Development Program EAVE (Experimental Autonomous VEhicle) (ref 3). One of these has been designed and fabricated at NOSC, and the other at the University of New Hampshire as a product of the Sea Grant Program. Both vehicles have "open-frame" construction, which is ideally suited to the pipeline and structures inspection requirements of hovering and maneuvering at zero and low-to-medium speeds. This type of construction also permits control and inspection sensors to be

added to the vehicle in the most advantageous locations. These sensors can also be readily changed to provide the optimum sensor package for a given mission task.

Characteristics of the two vehicles are shown in table 1. The vehicle actually chosen for demonstration of the fiber-optic communication link is the NOSC Free Swimmer, a photograph of which appears as figure 2. Detailed descriptions of the NOSC-developed EAVE WEST submersible are given in references 4 and 5.

| Characteristic/Capability | NOSC Submersible (EAVE WEST) | UNH Submersible (EAVE EAST) |
|---|---|---|
| PHYSICAL CHARACTERISTICS: | | |
| Length, ft | 9 | 5 |
| Breadth, inches | 20 | 5 |
| Height, inches | 20 | 3 |
| Dry Weight, lb | 400 | 820 |
| OPERATING CHARACTERISTICS: | | |
| Speed (max sustained still water), knots | 5 | 3.5 |
| Maneuverability, deg of freedom | 3 | 5 |
| Hovering Capability | Yes | Yes |
| Reverse Capability, knots | 3.5 | 3.5 |
| Mission Duration, h | 1* | 8 |
| Depth (max operating), ft | 2200 | 2000 |
| SENSORS/COMPUTER: | | |
| Control Sensors | Gyrocompass | |
| | Depth | |
| | Time | |
| | Leak detection | |
| | Altitude | |
| Data Sensors | TV camera & light | |
| | Magnetic pipe following | |
| | Super 8 movie & still camera | |
| | Acoustic pipe following | |
| COMPUTER CAPABILITY: | | |
| CPU | 8080 A | Intersil 6100 |
| ROM, kbytes | 20 | 1 |
| RAM, kbytes | 5 | 3 |
| Word length, bits | 8 | 12 |
| Clock | 2 MHz | 3 MHz |
| COMMUNICATION | Preprogrammable fiber optics | Preprogrammable acoustic |

*Extendable to 5 hours' duration by using lithium batteries in the same container space.

Table 1. Current characteristics and capabilities of the NOSC and UNH submersibles.

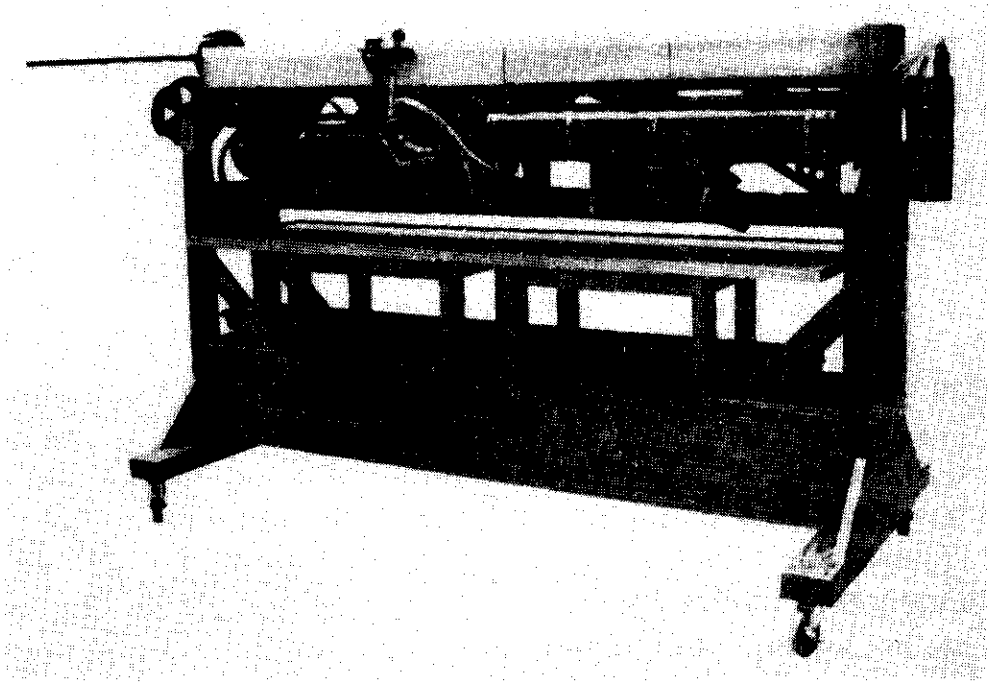

Figure 2. The NOSC/USGS free-swimming submersible EAVE WEST.

## 2.0 REQUIREMENTS

Requirements for the design and development of a fiber-optic communication link depend on both the operational requirements of the specific application for which the vehicle is designed and the general requirements which supervisory-controlled architectures impose. In addition, it is necessary to meet these requirements in a cost-effective manner. That is, the resulting system design must be cost-effective both to manufacture and to deploy and operate. If possible, the use of inexpensive "throw-away" fiber links should be considered. Above all, any design of a fiber-optically coupled vehicle system should be capable of demonstrating performance capabilities in both speed and maneuverability that approach those of a totally autonomous vehicle. The vehicle also should be capable of instituting automatic contingency procedures if the link fails.

### 2.1 OPERATIONAL REQUIREMENTS FOR UNDERSEA PIPELINE AND STRUCTURES INSPECTION

Operational requirements for a supervisory-controlled, unmanned submersible to be used for Outer Continental Shelf (OCS) inspection would be centered around the performance of the following inspection tasks:

1. The inspection of pipelines under US Geological Survey (USGS) jurisdiction for their geographical coordinates, for oil or gas leakage and, where exposed, for signs of deterioration in their concrete coverings.

2. The inspection of the submerged portion of offshore oil and gas platforms and other structures during and after installation for defects prejudicial to structural integrity such as cracks and bent, broken, or missing structural members.

Detailed inspection requirements for the vehicle documented in the EAVE program plan (ref 2) are as follows:

1. Pipeline Inspection Tasks.
   a. Conduct pre- and post-inspection mapping of areas of pipeline route to determine its geographical coordinates and pertinent terrain characteristics.
   b. Initiate inspection by locating specified starting point on pipeline.
   c. Navigate along, or track, pipeline with precision required by onboard sensors to perform their functions; the platform's maneuvering ability will permit stopping, maintaining position (hovering), and retracing pipeline.
   d. Observe, by means of onboard sensors, irregularities in pipeline condition; report these irregularities to a remote station and, upon command, perform a more detailed inspection or move to a new inspection area.
2. Offshore Structures Inspection Tasks.
   a. Locate structure, or a particular section of total structure to be inspected, after deployment in the approximate area.
   b. Navigate so as to trace structural members with precision required by onboard sensors to perform their functions; maneuvering ability will permit stopping, maintaining position (hovering), and retracing a structural member or network of members.
   c. Observe, by means of onboard sensors, gross structural irregularities and defects; report these irregularities to a remote station and, upon command, perform a more detailed inspection or move to a new inspection area.

Environmental requirements associated with the inspection tasks may be summarized as follows:

| | |
|---|---|
| Operating areas | OCS of the United States |
| Operating depth (max) | 2000 feet (near-term goal); 6000 feet (long-term goal) |
| Operating sea state (max) | As limited by support vessel |
| Current velocity at work site (max) | 2 knots. |

It has been determined that the potentially most useful application of a fiber-optic link in the offshore inspection scenario is that of pipeline inspection. In this application, the submersible can deploy the link along a relatively straight run with relatively little opportunity for entanglement of the line in the propellers or nearby features. Success will depend primarily upon the ability to deploy the link reliably with little or no drag.

A fiber-optically controlled vehicle for structures inspection promises to be significantly easier to maneuver than a tethered submersible with the same mechanical configuration and number of degrees of freedom. The stiff fiberglass-armored version of the fiber-optic tether promises to be less prone to breakage as a result of entanglement in the structure or with the vehicle propellers.

In high acoustic reverberation environments, such as shallow-water areas, the fiber-optic link promises to allow offshore inspections even when acoustic link systems would tend to be rendered ineffective by high error rates.

## 2.2 COMMUNICATION REQUIREMENTS FOR SUPERVISORY-CONTROLLED VEHICLES

The supervisory-controlled vehicle, as part of a closed-loop (in fact, man-in-the-loop) system, by definition requires a duplex communication link. This duplex link may be divided for discussion purposes into downlink (support platform to vehicle) and uplink (vehicle to support platform) communications. The former carries command-control information, while the latter, in addition to closing the command-control loop, also carries sensor information. Full duplex operation over a single optical fiber is readily achieved by the use of wavelength multiplex techniques, which obviate the need for cables containing more than one fiber.

Command-control information consists of obvious propulsion commands as well as the exchange of navigation and system status information (ie, depth, state of battery charge, etc). With the advent of the integrated circuit microprocessor, it is apparent that command-control functions are best carried out in a serial, digital format, and when so realized can be implemented readily via software. This approach excels in cost flexibility, effectiveness, and reliability. When microprocessors are employed, all synchronization, display, data transfer, time division multiplexing, and control are under the command of the processors. Reconfiguration of the system is easily accomplished by employing a universal data bus and simple software changes, which allow the vehicle to be quickly and efficiently reconfigured and optimized for the performance of diverse missions.

A proposed approach would place one microprocessor aboard the vehicle and another on the support platform. The former would locally manage affairs such as navigation, attitude compensation, homing and guidance functions, and the like, while the latter would oversee such functions as display and operator interfacing. The two units would communicate via UARTs (Universal Asynchronous Receiver/Transmitters), which would allow reprogramming and interaction as well as status reporting. The UART provides all formatting and synchronization to transfer data efficiently between the processors. Data transfer rates from 110 to 9600 baud are standard for such devices. Such an approach was adopted early in the design of the NOSC-developed EAVE WEST submersible.

Probably the single most valuable sensor for the inspection vehicle is a television camera. Such cameras, packaged and ruggedized for operation to depths of several thousand feet, are only slightly larger than a beer can and are available from several manufacturers. All such units employ standard composite video waveforms that satisfy RS-170 specifications. It is expected that the CCD (charge-coupled device) camera will soon become commercially available, and will allow a further reduction in camera size. Transmission of RS-170 real-time video requires a channel with a bandwidth of 2–5 MHz and a dynamic range of at least 40 dB. (Home-quality monochrome television occupies approximately 3.8 MHz with a dynamic range of 40–55 dB.)

Slow-scan converters are available which trade off frame rate, resolution, and dynamic range to decrease the required transmission bandwidth. For example, a commercial unit has been evaluated at NOSC which allows slow-scan television transmission via an acoustic channel with a bandwidth of only 3 kHz. One frame is transmitted every 8 seconds, and has a spatial resolution 20% that of RS-170 TV with 6% as much gray-scale rendition. Some applications may be tolerant of the loss of motion and resolution inherent in slow-scan TV.

In some instances, two or more simultaneous television channels may be desirable, perhaps to achieve a visual stereo effect, and thus the bandwidth requirement of the transmission channel will be increased. Real-time TV probably has the highest bandwidth requirement of any sensor likely to be employed with an undersea inspection vehicle, and as such will drive the system bandwidth requirement.

Sonar is often employed as a sensor on undersea vehicles to extend the viewing range greatly over that obtainable by using television, but with a corresponding reduction in resolution. Both front-looking and side-looking units have been employed. Such sonars require channel bandwidth that range from perhaps 10 kHz to more than 500 kHz, depending on capability. The dynamic range required is on the order of 20 to 30 dB.

Such sensors as magnetometers and fluorometers undoubtedly will be desirable on some vehicles, especially those used for pipeline inspection. Data from these low-bandwidth sensors is best transmitted digitally, with expected data rate requirements of only a few bits per second. This class of sensor information is best transmitted by allowing the microprocessor controller to incorporate it, along with such data as compass heading and depth, via the UART command-control link.

Akin to sensors are manipulators, which range from simple claws to sophisticated tactile, force-feedback units. It is possible that the inspection vehicle will contain some form of manipulator which will allow it to attach markers and lines to points of interest. A supervisory-controlled manipulator soon will be installed on the EAVE WEST submersible as one of the other technologies that are being investigated as part of the EAVE Program (ref 5 and 6). Manipulators can, like low-rate sensors, be accommodated via the UART link, although the more complex units will probably require the 9600-baud rate to minimize time lag in the control loop.

In the fiber-optically coupled free swimmer, therefore, it is obvious that the communications link must be duplex; this can be realized by the use of different wavelengths or light for the uplink and downlink signals. The downlink will be digital PCM (pulse code modulation) via a UART operating at 9600 baud to maximize the data transfer rate and provide for manipulator control. The uplink will carry an identical UART channel as well as a monochrome television channel requiring a bandwidth of approximately 4 MHz. The UART channel can be readily time-division-multiplexed into the blanking interval of the television channel. In addition, missions may require color and/or stereo television sensors, which will increase the bandwidth even more. Finally, a sonar channel having a bandwidth requirement which is a small fraction of that required for television may be mandated if visibility range in excess of that obtainable with optical techniques is required.

## 3.0 SYSTEM REALIZATION

We will now attempt to address the specific areas of investigation which are required to develop a total system suitable for use on the EAVE WEST submersible for OCS pipeline and structures inspection. In each of these areas, it was necessary to make choices that best suited the OCS inspection application (which may not necessarily be the same choice desirable for military applications). For example, the desire to investigate the use of an unarmored fiber link, which would be a low-cost, throwaway item, was important to the OCS scenario, in which the operational cost for inspections is important. On the other hand, such items as spool fabrication techniques and modulation and multiplexing techniques obviously have a wide area of application for all types of underwater operations.

## 3.1 DEPLOYMENT CONCEPT

The present deployment concept for a fiber-optic supervisory-controlled submersible calls for paying out an optical fiber tether cable from a vehicle-mounted prewound, pretwisted, stationary free-standing spool as the vehicle moves along its underwater path. Once the cable leaves the spool, the intent is not to have the vehicle pull it through the water but rather to have the tether lie relatively motionless in the water column. Thus, in concept, the vehicle with its spool of cable will move through the water column while laying its tether in its track. This concept assumes that the link ultimately will be low enough in cost to be expendable. To achieve this cost, the intrinsic expense of the cabling process associated with the packaging of the optical fiber must be low. In addition, if it is to be capable of extended track ranges, say 10 km, the cable must be small and light because of packaging and payload limitations. The only strengthening allowed, therefore, is the minimum required to permit the cable to be handled and deployed without breakage for the duration of the intended mission; typically on the order of several hours. In addition, the tether deployment mechanism must be inexpensive and reliable.

### 3.1.1 FIBER-OPTIC LINK

To achieve desired design objectives, several low-loss optical fiber link designs are presently under consideration. The physical characteristics of each generic type are listed in table 2. A Mk 37 torpedo wireguide is also listed for comparison purposes.

Design 1, the "unarmored fiber-optic element," consists of the glass optical fiber surrounded by a polymer buffer layer which prevents surface abrasion and a resulting weakening of the glass (see figure 3). Essentially, all the tether's strength is provided by the glass itself; for a 0.005-inch-diameter fiber proof-tested to a stress level of 200 000 psi, a proof strength of approximately 4 pounds results. The buffer layer increases the total tether diameter to approximately 0.020 inch. Experimentation with winding and deployment of this fiber cable has shown that such an unruggedized design is not practical. A cable design with no stiffness other than that provided by the 5-mil-diameter fiber must be wound or spooled with a binding agent of extremely low adhesive strength such as lacquer or rubber cement. Unfortunately, binding agents of this type create a very slow winding rate and result in a structurally unstable package from a handling standpoint. In addition to practical spool fabrication problems, the unruggedized cable design may not necessarily result in the lowest cost, as might be assumed. The reason is that a high proof-test specification of 150–200 kpsi results in a very high cost per meter for long, continuous (5000-m) lengths. For example, in FY 80, 5–km lengths of 100–kpsi proof-tested fiber were bought from ITT for $1.25/m. ITT would not bid on fiber of this length at higher proof tests, or at a 100–kpsi proof test in longer than 5–km lengths. Sumitomo, on the other hand, supplied 5–km lengths of fiber proof-tested to 150 kpsi for $2.50/m. The capability of the optical fiber manufacturers to supply fiber to high proof tests, low loss, and great lengths is characterized by "yield" curves. Such a family of curves is depicted in figure 4. Note that these curves vary from one manufacturer to another and are determined by the level of manufacturing technology attained by the company.

Payout experiments in FY 80 determined that a stiff tether was required to bend-limit the cable at the spool peel-off point. In addition, a minimum tensile strength of 6–10 lb would be required to achieve a reasonable safety factor. For these reasons, it became apparent that some sort of "ruggedization" would be required for the cable. A standard

| Item | Mk 37 Wire | Unarmored Optical Fiber (ITT or Sumitomo) | Ruggedized S-glass Optical Fiber | Minimally Cabled Kevlar Optical Fiber* |
|---|---|---|---|---|
| Outer Diameter, inch | 0.053 ± 0.003 | 0.18 ± 0.002 | 0.036 | 0.040 ± 0.001 |
| Density, $lb/ft^3$ | 99 | 82 | 108 | 127 |
| Weight in Seawater, lb/ft | $6.83 \times 10^{-4}$ | $3.27 \times 10^{-5}$ | $3.13 \times 10^{-4}$ | $5.5 \times 10^{-4}$ |
| Specific Gravity | 1.58 | 1.32 | 1.73 | 2.03 |
| Breaking Strength, lb | 20 | 2–4 | 50–80** | 250 |
| Recent Price per ft (1979) | -- | $0.25–2.50 | $0.75–1.75 | $2.50 |
| Bandwidth | | | | |
| Commercially Available | 10 Hz/km | 0.5 GHz/km | 0.5 Hz/km | 0.5 Hz/km |
| State of the Art | 10 Hz/km | 2 GHz/km | 2 Hz/km | 2 Hz/km |

* This approach is clearly judged to be unfeasible because of storage volume requirements and cost constraints.

**High value is based on calculations made by means of known material properties. Low value is based on a scaling of data from a 0.040-inch-OD, 32-end S-glass cable.

Table 2. Candidate tether material characteristics.

graded-index (GI) optical fiber from ITT was chosen as a baseline component. Previous cable development work done by NOSC, Hawaii, had resulted in a "ruggedized" optical fiber cable design that had an OD of 0.040 inch and a usable tensile strength of 90 lb when an optical fiber proof-tested to 1% strain was used. To fabricate this cable, a 5-mil, low-loss, high-strength (minimum 1% proof test) optical fiber is drawn and a protective buffer composed of silicone RTV is dip-coated onto the fiber to produce an OD of about 12 mils. Then a harder, nontacky plastic such as HYTREL is extruded onto the silicone layer until a 20-mil diameter is achieved. These buffer coatings are added during the fabrication of the fiber to protect it from abrasion and microbending. The glass fiber yields a "weak-link" strength of approximately 2 lb in tension when proof-tested to a 1% strain or 100-kpsi load specification. Developmental efforts during FY 80 determined that the buffered fiber as supplied by the manufacturers had insufficient strength and stiffness for reliable deployment. To eliminate this problem, "S-glass ruggedizing" can be used. The S-glass armored configuration is made by laminating an epoxy resin and S-glass filament composite over the original HYTREL jacketed fiber, increasing the OD to approximately 35 mils. The S-glass matrix is laid parallel to the optical unit to achieve maximum strain relief and to eliminate torque while the cable is under tension. The result is a usable tensile strength of approximately 60 pounds (using 1% proof-tested fiber) and a degree of built-in stiffness that tends to prevent cable breakage at the peel-off point on the inner layer. Figure 5 shows the cable cross section.

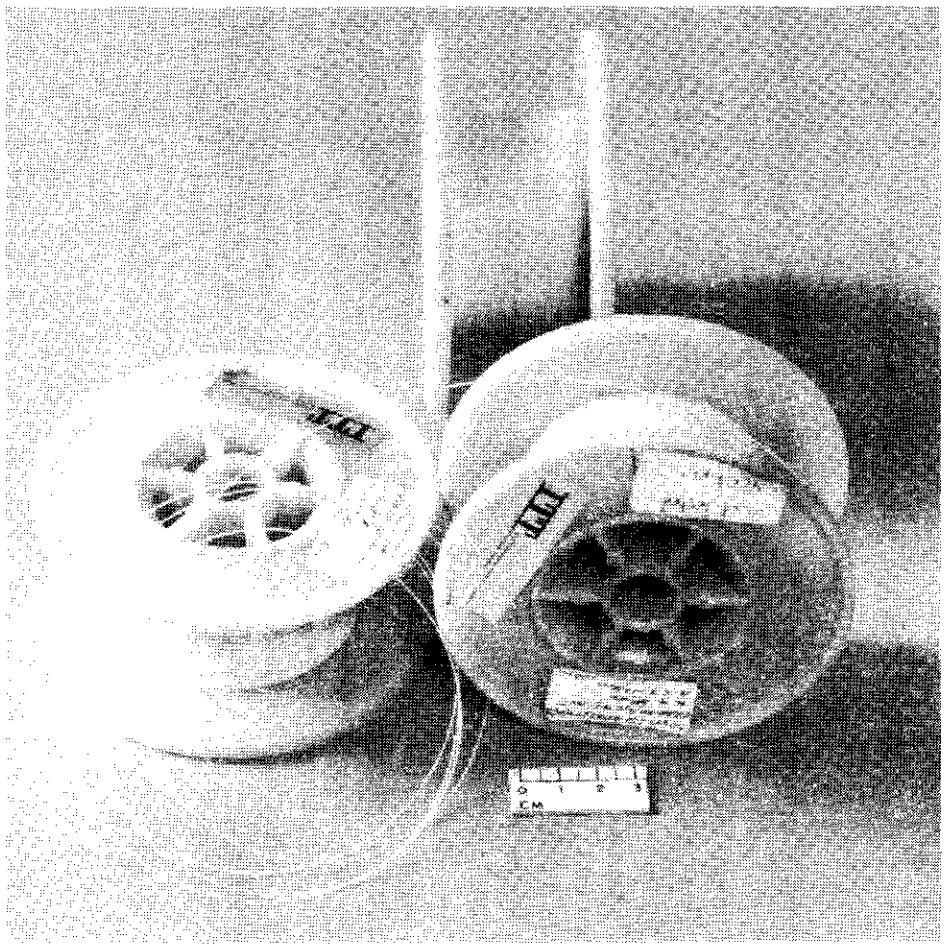

(A) MANUFACTURED BY ITT.

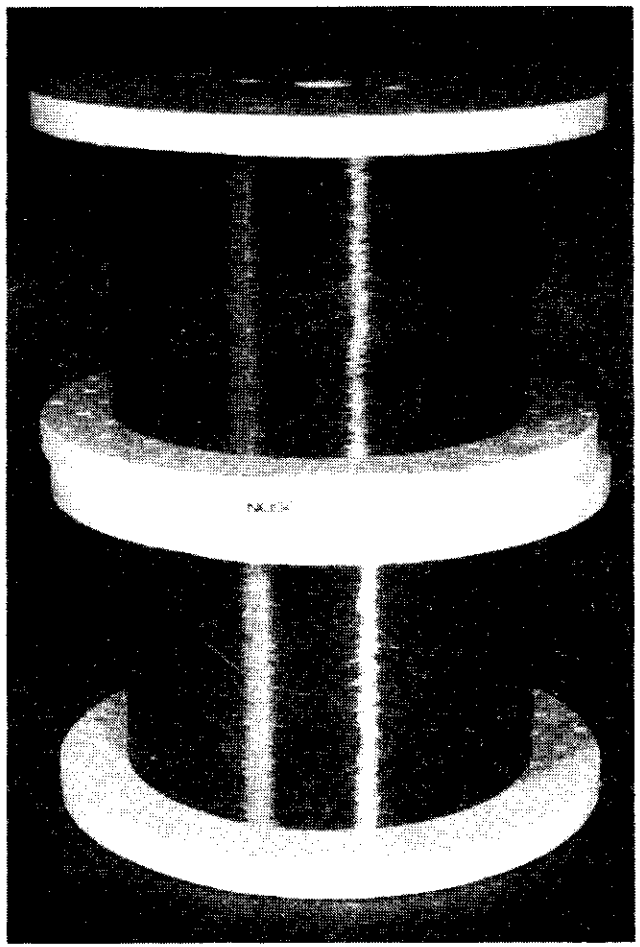

(B) MANUFACTURED BY SUMITOMO ELECTRIC, JAPAN.

Figure 3. Design 1; the unarmored fiber-optic element.

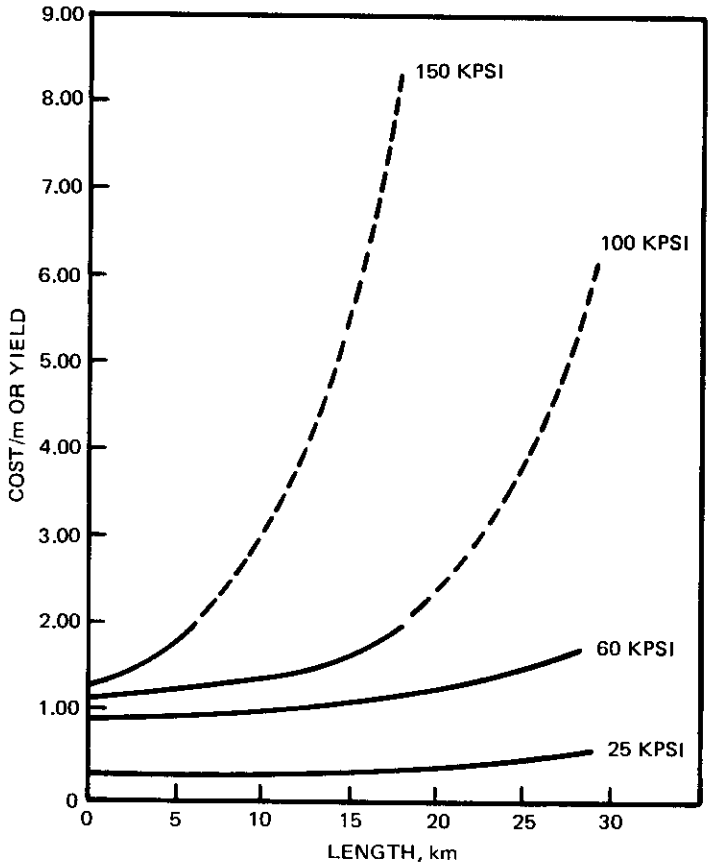


Figure 4. Typical yield curves for fiber-optic links.

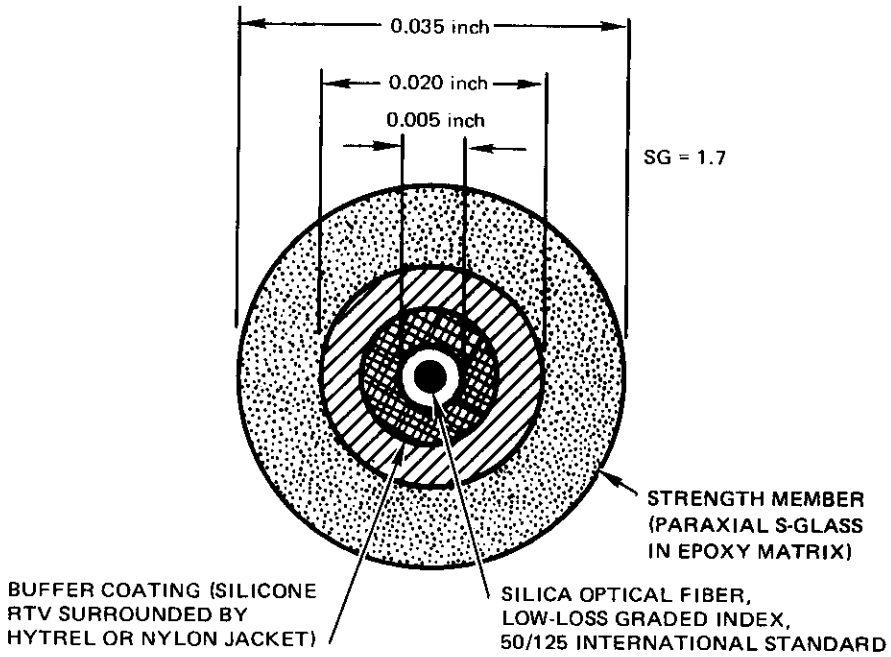


Figure 5. Cross section of the S-glass armored fiber link.

### 3.1.2 DEPLOYMENT TECHNIQUES

Deployment of the cable is accomplished by a center pullout technique from a prewound stationary spool. The pullout deployment concept requires that the cable unwind from the ID of the spool. To avoid snagging and breakage in the payout guideway, it is imperative that the cable free itself from the binding agent/cable matrix that makes up the spool in a highly uniform manner. One key to achieving this uniform payout is the selection of an inside payout technique, in which the cable breaks free from the inner wall of the spool and has an unobstructed path to the payout tube.

### 3.1.3 SPOOL FABRICATION CONSIDERATIONS

A prototype, manually operated, fiber-optic winding machine was developed and used to wind a number of trial spools for preliminary feasibility tests during FY 78. Several 100-meter lengths of unarmored, plastic-buffered optical fiber elements, proof-tested at a 400-kpsi level, were wound with a pretwist so that upon deployment the fiber would not kink. An adhesive was manually applied to provide a binding force such that pullout required about 1/10 lb. Several binding agents were qualitatively evaluated, including waxes, aerosol rubber cements, and lacquer. A deployment experiment was conducted in an underwater test tank where the fiber was deployed at rates up to 18 knots without breakage.

These initial tests demonstrated the feasibility of the deployment concept, but left open the questions of which tether design and which binding agent need to be used in an actual application and also underscored the length-versus-strength tradeoffs which become critical concerns with long fibers because of their impact on mission costs. The preliminary fabrication/deployment work showed that it is possible to use this approach in the laboratory. However, the initial work also showed that it takes 3 to 4 hours of a technician's time manually to wind 100 meters uniformly. Thus the winding process was subsequently automated and expedited to make the spool/package inexpensive. It became obvious after some experience that extreme flexibility in altering the winding parameters would be necessary in follow-on efforts if pertinent questions were to be addressed and solutions found.

To fabricate the spools, a microprocessor-controlled winding machine is now used to position each coil precisely as it is wound on the takeup mandrel (fig 6). Synchronously, as each coil is formed, a 360-degree pretwist is applied. As the cable goes onto the mandrel, the adhesive is applied to fix each coil relative to the other coils in an in-line process. The machine currently is capable of winding 5 km of 35-mil-OD cables. Because the guide head movement or advance is controlled by the microprocessor, any diameter of cable can be wound with a simple change in the control program. The machine is presently capable of winding 1 km of cable in less than 3 hours. Changes to the software and the motor drive units will increase this rate to less than 1 km/hour for a 10-km spool.

The microprocessor-controlled winding machine made spool fabrication practical and at the same time very flexible. For the EAVE WEST submersible, a standard spool ID of 5 inches was chosen because of optical loss considerations. A sample 500-ft deployment spool fabricated automatically by this machine for the EAVE WEST vehicle is shown in figure 7. The deployment canister and standoff stinger used on this submersible are shown in figure 8.

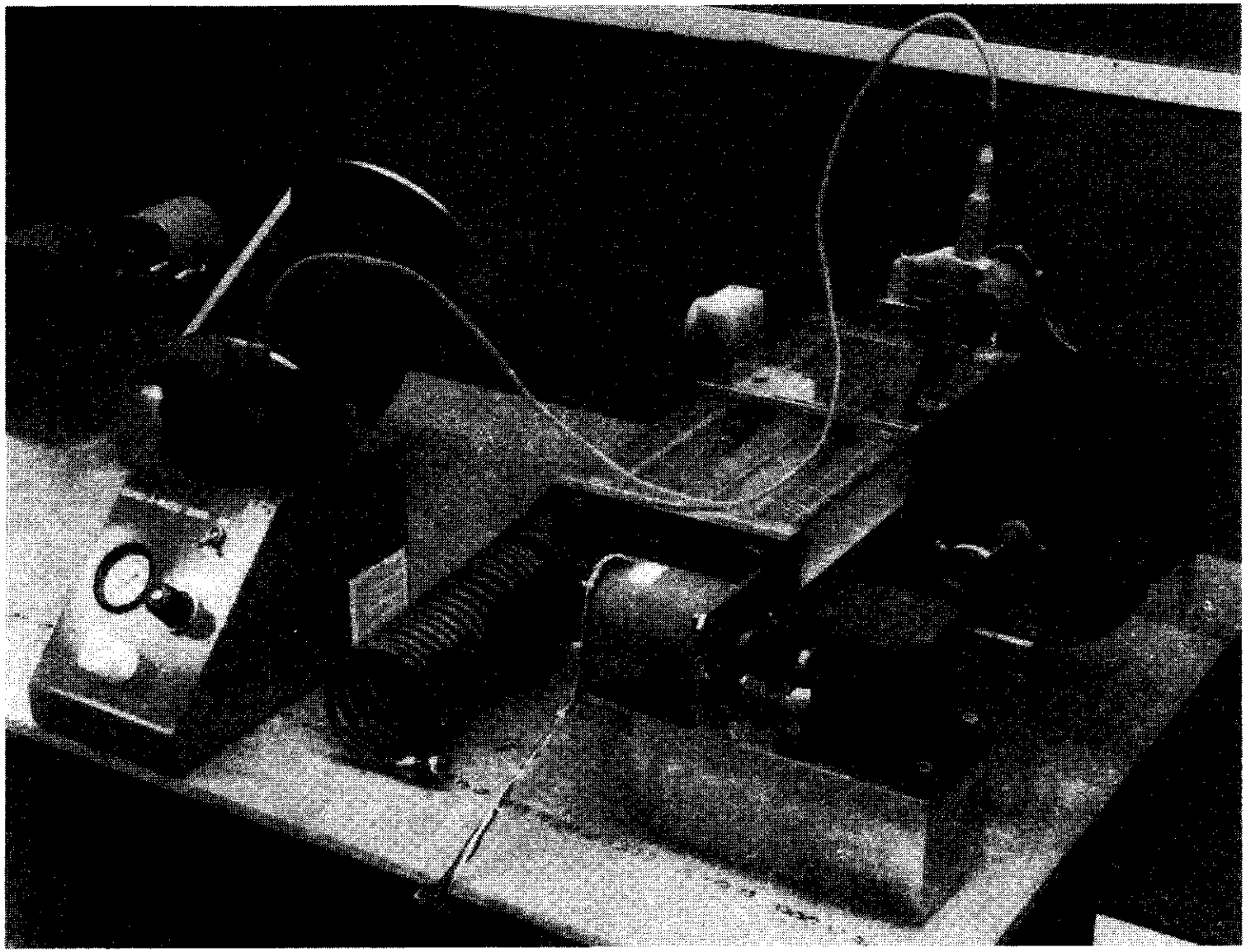

Figure 6. The microprocessor-controlled optical fiber winding machine.

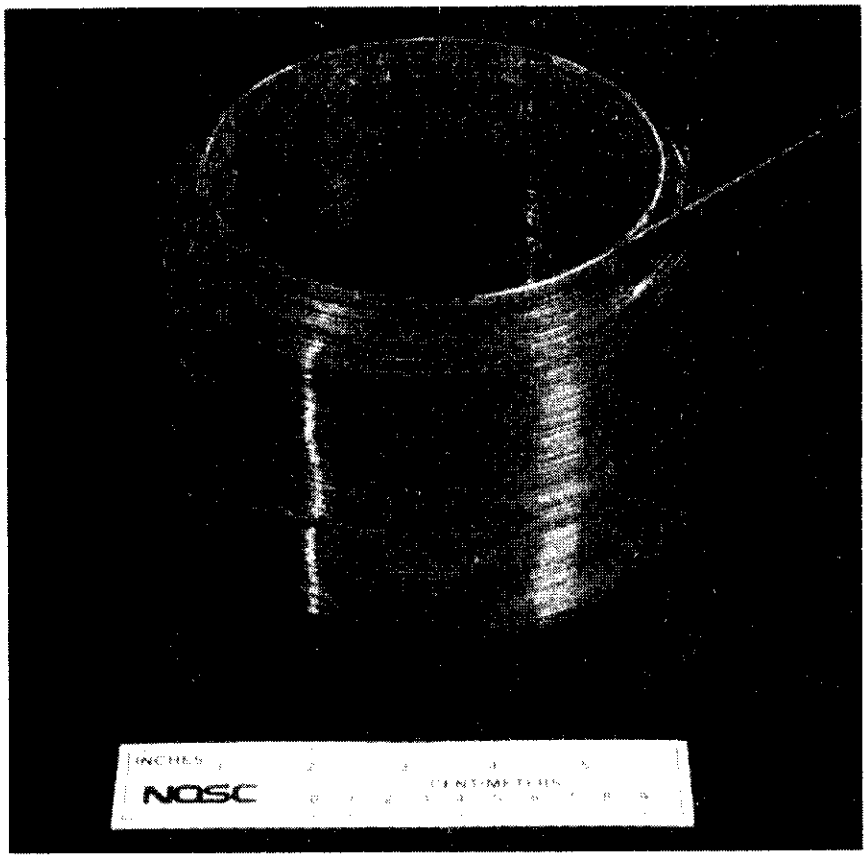


Figure 7. Design 2; the ruggedized fiber (S-glass) as wound on a deployment spool.

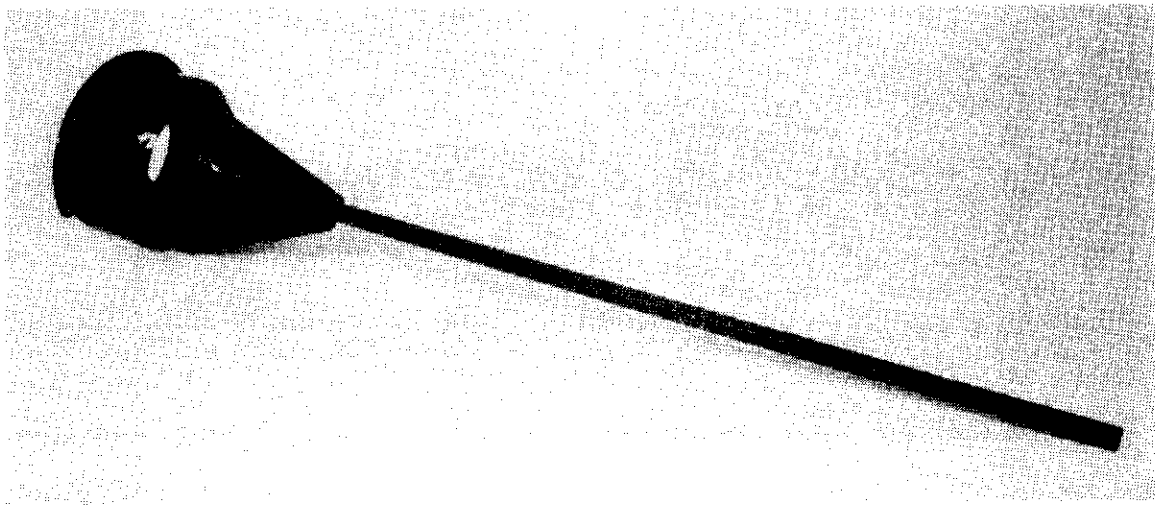

Figure 8. The fiber-optic deployment canister used on the EAVE WEST submersible.

Gloge (ref 6) writes of radiation loss and mode coupling induced by curvature of the fiber. A relationship that determines attenuation loss of a given mode as a function of bend radius for a two-dimensional analysis is given by:

$$\alpha = 2\,nk\,(\theta_c^2 - \theta_c\theta)\exp\left[-2/3\,nk\,R\,(\theta_c^2 - \theta_c\theta) - \frac{2a}{R}\right]^{3/2}$$

where

$\alpha$ = attenuation for mode defined by $\theta$ in dB/km in graded index fiber

n = index of refraction at core of fiber

k = free space propagation constant = $2\pi/\lambda$

$\lambda$ = wavelength of light in m

$\theta_c$ = critical angle of waveguide = $(2\Delta)^{1/2}$

$\Delta$ = index difference of cladding and core

a = radius of fiber core in m

R = radius of bend curvature in m.

Assuming a fiber with core radius of 25 $\mu$m, an index of refraction of 1.5 at the core, an index difference of 2% between core and cladding, and propagating light of a 1-$\mu$m wavelength, the bending loss for a mode can be calculated as a function of bending radius. Figure 9 is a plot for several modes as an illustration of the sensitivity of these modes to curvature. For a given mode, the loss increases logarithmically with bend radius. In general, it is primarily the high-order modes that are lost and this is borne out by the calculated numbers. However, the mechanism of mode coupling works to replenish these high-order modes with lower-order mode energy in an effort to reach mode equilibrium in the waveguide. Thus a spool of fiber composed of a multitude of coils presents a structure that induces an additional, continuous loss. The attenuation numbers in figure 9, however, suggest that by limiting the bend radius to a large value, bending losses can be kept to a very low level. Gloge determined that a graded-index fiber would lose a proportion of its transmission modes equal to

$$y = 2a/R\Delta.$$

Therefore, the radius at which one-half of all modes is lost is equal to 0.5 cm. Based on this analysis, a minimum spool-winding diameter of 5 inches was selected as a compromise between packing efficiency and low bending loss.

Given a close-packed, precision-wound spool, the OD and length of the spool can be related by the following equation:

$$L = \frac{4\,\ell d^2\,(\cos 30^\circ)\,39.36}{\pi\,(OD^2 - ID^2)}$$

where

L = spool length in inches

$\ell$ = cable length in km

d = cable diameter in inches

OD = outside diameter of spool in inches

ID = inside diameter of spool in inches.

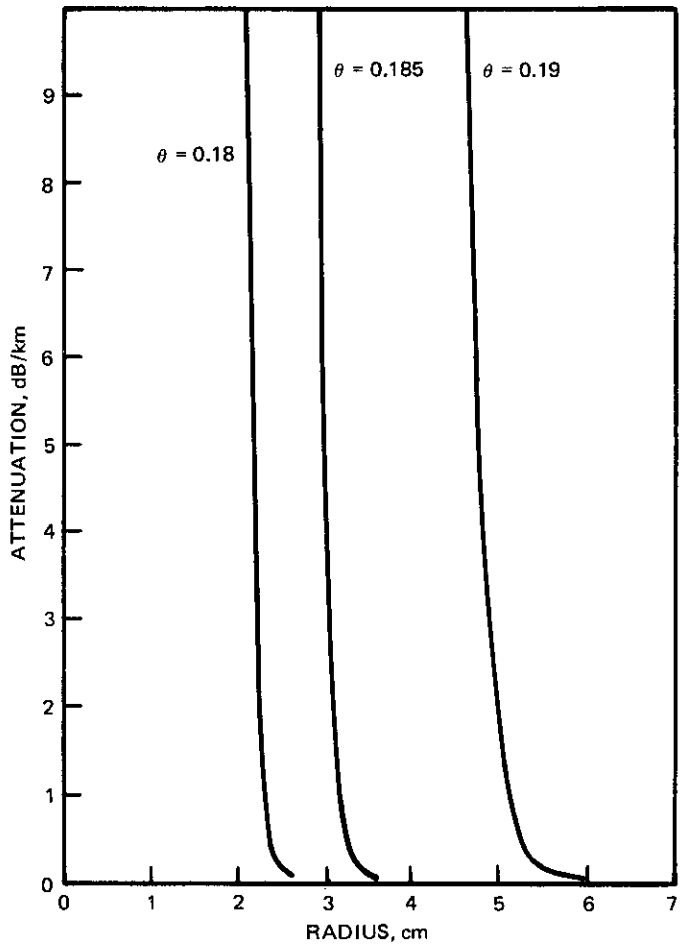


Figure 9. Sensitivity of various modes to curvature.

Figure 10 is a plot of spool length as a function of OD given an ID of 5 inches and cable lengths of 5 km and 10 km. Plots are shown of cables of several different diameters to show the effect of a slight reduction in cable diameter on the spool volume.

### 3.1.4 PROGRESS TO DATE

Several key cable measurements were done in FY 80. These included

- Attenuation changes attributable to ruggedizing the bare fiber to the finished cable form.
- Attenuation change attributable to precision-winding the cable into a self-standing spool.
- Attenuation changes attributable to operating pressure levels.
- Excess attenuation during payout attributable to bending at the peel-off point.

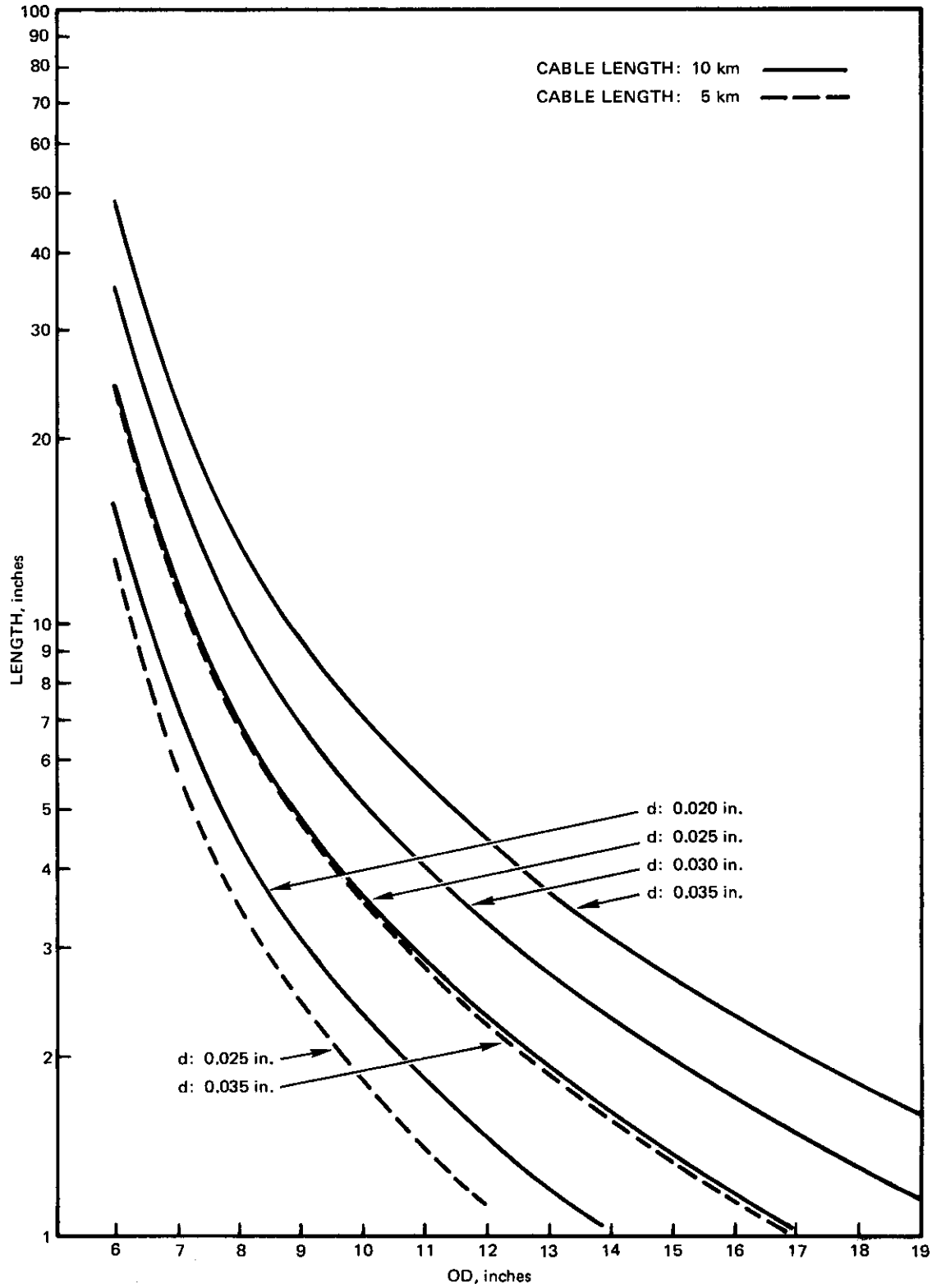


Figure 10. Plot of spool length as a function of OD with an ID of 5 inches and cable lengths of 5 and 10 km.

In the fourth quarter of FY 80, 8 km of ruggedized facsimile cable was wound, payed out, and filmed with high-speed photography. The facsimile cables allowed us to check the winding/fabrication technique of the spools and also the payout test procedures without wasting expensive fiber-optic-cored cables. Payout tests of the facsimile cable proved that the adhesive was of sufficient strength for packing the stiff cable and yet yielded only about 0.5 lb of tension at payout speeds of 10–65 knots. In parallel with the payout work, two 1-km lengths of ITT fiber were ruggedized. Attenuation measurements before and after ruggedizing indicated no measurable change in loss. Each 1-km length of ruggedized cable was then precision-wound at the NOSC, San Diego, facility. One spool was taken to NOSC, Hawaii, and pressure-tested to 7000 psi while the attenuation was monitored. The other spool was taken to the Naval Underwater Systems Center, Newport, for payout tests where both attenuation and tension could be monitored. At a 1000-psi pressure, excess attenuation of 0.1 and 0.6 dB/km at 0.83-$\mu$m wavelength was detected on the different tests. The spool remained structurally intact after being subjected to as much as 7000 psi. There was no permanent damage to the optical fiber at 7000 psi since attenuation measurements conducted many days after pressurization showed no significant change in the baseline loss characteristics. The payout tests were done at speeds from 10–65 knots and no detectable increase in attenuation resulted from payout stresses. Attenuation measurements on the cable before and after ruggedizing and winding showed no adverse attenuation effects from either process. Temperature cycling tests on the cable are planned for early FY 81.

### 3.1.5 FUTURE WORK

Work to date has shown that an expendable fiber-optic cable of small size can be deployed reliably at speeds from 10–65 knots. Lengths as great as 4 km have been ruggedized, wound, and successfully payed out. In achieving this, it has been found that some ruggedization has been necessary to provide bending stiffness and added tensile strength to the bare optical fiber. Excess attenuation attributable to pressure has been found to be small at pressures up to 1000 psi, and to increase rapidly to unacceptable levels at pressures beyond 2000 psi. No excess attenuation was detected because of dynamic stresses on the cable during payout. The ruggedization and precision winding of the optical fiber had no measurable effect.

Future work will be directed at eliminating the pressure sensitivity of the cable as well as any adverse temperature effects. An effort also will be made to reduce the size of the ruggedized cable. This will result in a much better volumetric efficiency for the optical link. The goal will be a 25-mil-OD cable.

To reduce cable cost, an effort will be made to reduce the tensile strength of the fiber to a level that can be compensated for by the ruggedizing layer. The goal will be to achieve a 10–20-pound tensile proof load on the composite cable. In a further effort to reduce dramatically the mission cost of the cable, it is believed that the USGS program should investigate the possibility of reusing the cable for several missions. The major disadvantages of this approach are the decreased reliability of the link with each use and the requirement to reprepare the cable for winding. However, it should be noted that a USGS inspection mission is not a weapon delivery situation, and that reuse of the cable can be facilitated by incorporating a thin, say 1-mil-thick, layer of Hytrel around the ruggedizing material so that the spooling provides a bond between the plastic layers rather than the ruggedizing material. During deployment, the plastic sheath would become a tear-away layer, leaving the deployed cable relatively clean and readily reusable. It is estimated that the cost of re-extruding the plastic layer will be minimal. Future developments in splicing the ruggedized cable also will tend to make this multiple-use concept more attractive.

## 3.2 MISSION SCENARIO IMPACT AND TETHER DYNAMICS

While the fabrication process influences the selection of cable design and the binding force of the adhesive, the mission scenario, which includes such factors as current profile and standoff considerations, also affects the selection process. The pullout force required will be set by the binding agent or its equivalent (note that the final design option may call for a mechanical pullout-limiting device and the use of a minimal-binding-force adhesive). Different binding forces on the reel could produce minimum pullout tensions ranging from nearly zero up to the breaking point of the tether. (Such wide ranges are easily produced through the use of cyanoacrylate adhesives.)

Payout reels are envisioned on both the support vessel and the tethered underwater vehicle. The canister on the support vessel would pay out tether to compensate for heave and other ship movements. The reel on the tethered vehicle would pay out cable as the vehicle moves in the water and as the drag pulls it out to form a catenary. Differential pull-out tensions would affect the scope in such a catenary. A too-large binding force and the resulting pullout tension would tend to inhibit catenary formation. Conversely, a too-small binding force would tend to permit the excessive deflection of tether by current in the water column.

The choice of a tether design and the magnitude of the binding force required as a result is considered important to the overall design for a specific application. The tension on the tether and the amount of catenary to be formed during deployment could be determined by extensive laboratory and sea tests, but the cost of such tests would be prohibitive. It was decided instead to construct a mathematical model by means of finite element analysis to predict the behavior of the fiber-optic tether during deployment. The calculations necessary for the model are performed on a computer, and the results assist the mission planner in choosing the proper cable type and profile for a given scenario (see appendix).

## 3.3 MODULATION AND MULTIPLEXING TECHNIQUES

Using a fiber-optic data channel to link an undersea vehicle with its support platform allows high-bandwidth, low-noise, real-time communications vital to many missions. Typically, such a link is required to transmit one or more television channels, sonar video, and command/control information. The optimum fiber-optic transmission system for such applications must be capable of repeaterless operation despite high optical cable loss, must satisfy realistic optoelectronic and fiber bandwidth constraints, and must have low signal distortion, minimal power consumption, a straightforward hardware realization, and low cost. Traditional digital and linear analog fiber-optic modulation techniques, when applied to video-bandwidth signals, fall short of satisfying these requirements.

### 3.3.1 THEORETICAL DISCUSSION

A nonlinear analog modulation scheme, pulse frequency modulation (PFM), has been shown to be suitable for the transmission of video-type signal information (ref 8). Investigations at NOSC have involved characterization of the processing gain obtainable with this technique, and resulted in a set of design equations that predict system performance and allow the designer to optimize parameters to suit his particular requirements (ref 9 and 10). In conjunction with the theoretical analysis, the Center has developed prototype fiber-optic

hardware specifically designed to accommodate the functions required of an undersea vehicle television data channel. The hardware utilizes PFM transmission by means of a light-feedback stabilized injection laser diode transmitter and an AGC-controlled avalanche photodetector receiver. The equipment exhibits a maximum loss margin of nearly 60 dB for transmission of a 4.5-MHz bandwidth composite television signal, which translates to an unrepeatered cable length in excess of 15 km with currently available optical fibers operating in the 0.85-$\mu$m spectral band. Laboratory-grade research components recently have demonstrated that repeaterless transmission range can be extended to more than 50 km by switching to the use of longer infrared wavelengths in the 1.2–1.6-$\mu$m band. Figure 11 depicts a simplified block diagram for a fiber-optic data link that employs PFM.

A data source (ie, pre-emphasized composite video) is applied to a voltage-controlled oscillator (VCO) to provide a narrowband FM signal whose carrier frequency is slightly in excess of the Nyquist rate. A pulse former is triggered from zero crossings of the narrowband FM waveform to yield a train of narrow, constant-width pulses whose period varies as a function of the instantaneous data signal amplitude. This pulse train is subsequently transmitted through the optical fiber by means of an optical transmitter that employs a semiconductor injection laser. Note that the PFM transmitter has, in effect, mapped signal amplitude into time differences – it is the time spacing between successive optical pulses in the PFM waveform that carries the signal information.

The light signals transit the optical fiber and are reduced in amplitude (attenuation) and spread in time (dispersion). The optical pulses, upon reaching the end of the fiber, are converted into electrical current by a photodetector which additionally broadens the pulses (by virtue of its internal multiplicative gain and/or electronic preamplifier thermal noise). The broadened, noise-corrupted pulses are then reconstituted by a comparator into a pulse train similar to that which was transmitted. The effect of dispersion and noise is to add a degree of jitter to the reconstructed pulses, thereby degrading the ultimate time recovery accuracy obtainable. It is shown in ref 9 that, if system operational parameters are correctly chosen, the effect of this jitter is insignificant on the quality of a television picture. A video bandwidth low-pass filter follows the pulse reconstructor, which restores the baseband signal by rejecting the RF components, thus forming a time-averaged discriminator (ref 11).

It is helpful to consider a frequency domain representation of the preceding technique to understand the nature of PFM processing gain. The action of the transmitter is to expand the signal bandwidth occupancy, then to map amplitude into time. More bandwidth is necessary to transmit the train of narrow pulses than would be required to convey the baseband signal itself. It can be shown that the spectrum of PFM is composed of a series of harmonically related, phase-locked FM spectra having theoretically infinite bandwidth (ref 12). Each subspectrum has an FM modulation index proportional to the order of its local

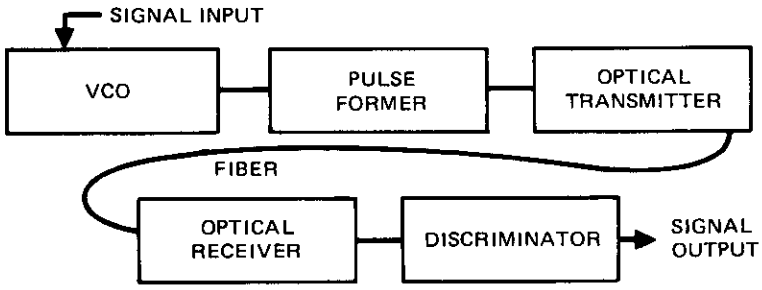


Figure 11. Basic PFM transmission scheme.

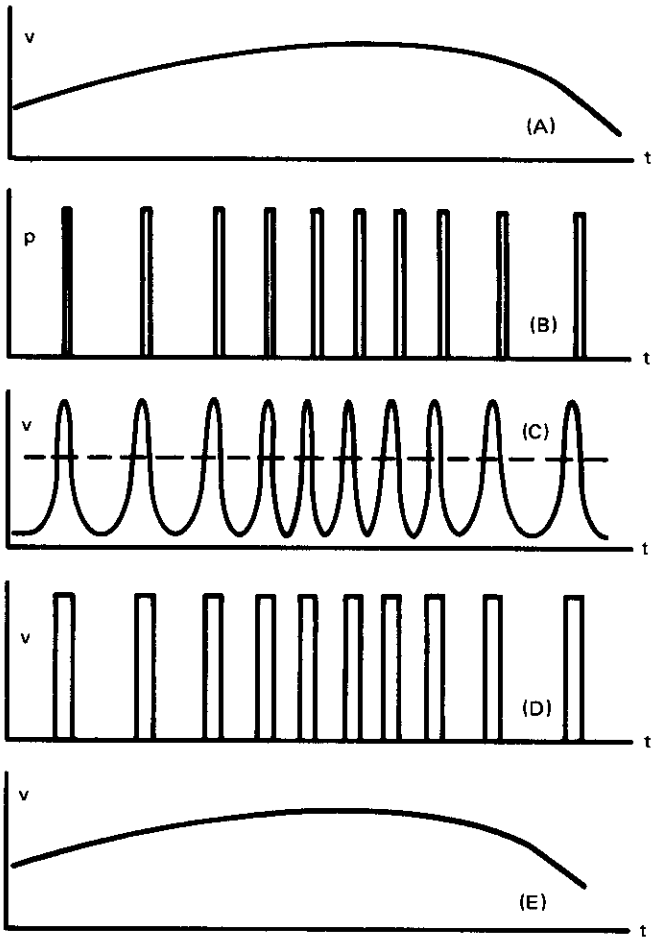


(A) MODULATING WAVEFORM.
(B) PFM WAVEFORM TRANSMITTED OPTICALLY.
(C) RECEIVED PFM WAVEFORM SHOWING EFFECTS OF BANDLIMITING AND NOISE. COMPARATOR SLICING LEVEL IS SUPERIMPOSED.
(D) RECONSTRUCTED PULSE TRAIN FROM SLICER.
(E) RECOVERED TRANSMITTED WAVEFORM AFTER FILTER.

Figure 12. Waveforms encountered in the PFM system.

carrier frequency divided by the pulse train center frequency. The frequency-expanded PFM signal can efficiently take advantage of the wide overall bandwidth capability of fiber-optic transmission. At the receiver, noise is added and the signal is effectively frequency-compressed by the discriminator back to its original bandwidth. Because the signal components in the PFM spectrum are correlated (ie, add up in the time domain to a time-varying pulse train) and the noise components over the band are not, the signal components add coherently upon detection and the noise power adds in a noncoherent manner, which yields a net processing gain. This is entirely analogous to well known modulation formats such as FM and PCM, which increase postdetection signal-to-noise ratio at the expense of predetection transmission bandwidth.

### 3.3.2 HARDWARE REALIZATION

The NOSC prototype brassboard PFM data link (fig 13) is designed to be installed on the EAVE WEST testbed submersible described earlier (fig 2, ref 4 and 5) to demonstrate the concept of a supervisory-controlled undersea vehicle with an expendable fiber-optic data tether. The link features a 4.5-MHz-bandwidth RS-170 television signal (uplink only) and a pair of 9.6-kbaud asynchronous microcomputer RS-232 digital PCM channels (duplex). The uplink computer data are time-division multiplexed onto the television horizontal sync pulses to form a composite signal, and this signal is PFM-encoded for transmission to the surface at a wavelength of 0.84 $\mu$m. The 9.6-kbaud downlink channel is color-multiplexed onto the same fiber used for the uplink at a wavelength of 1.06 $\mu$m and transmitted by means of PCM. Dichroic beam-splitter couplers developed by NOSC serve to separate the wavelength-multiplexed signals at the ends of the link (ref 13).

The PFM transmitter is composed of a prebiased, low-threshold injection laser, a light-feedback laser stabilizer, and a PFM modulator (fig 14). The laser couples 5-mW light pulses into 50-$\mu$m-core, graded-index optical fiber.

The PFM receiver (fig 15) consists of an avalanche photodetector (APD) with a cascode transimpedance front-end preamplifier. The electrical pulse amplitude is maintained at a relatively constant level independent of optical levels (ie, cable lengths) by a dual-loop AGC feedback circuit which controls both the gain of the APD and the gain of a postamplifier stage. In this manner, the APD avalanche gain is maintained near optimum for a wide range of input levels. A feedforward ALC voltage is applied to the level comparator which maintains the decision threshold at one-half the peak pulse height for maximum discrimination against jitter. Near threshold, the decision level is automatically increased to 70% of the peak level to extend the system threshold. The one-shot multivibrator and low-pass filter comprise a pulse-averaging discriminator with very wide dynamic range and excellent linearity. The receiver ROC (receiving operating characteristics) are depicted in fig 16 and compared with theoretical predictions.

### 3.3.3 PROGRESS TO DATE

It has been shown analytically and verified experimentally that PFM is a high-performance modulation technique when applied in conjunction with fiber-optics technology. Equations have been developed which model the specific application (ref 9 and 10). PFM has been compared with more conventional fiber-optic modulation techniques, IM and PCM, and offers many operational and performance advantages – particularly in the context of application to the long undersea vehicle tether cables required to transmit video bandwidth information. Finally, a brassboard PFM optical transmitter/receiver set has been designed, tested, and evaluated in the laboratory. All that remains is installation of the system on the EAVE WEST submersible and testing of the entire system at sea.

## 3.4 UNDERWATER HOUSING PENETRATION TECHNIQUES

The fiber-optic pressure penetrator is a key component required to implement a fiber-optic communication link on a free-swimming vehicle. In addition, such devices will be

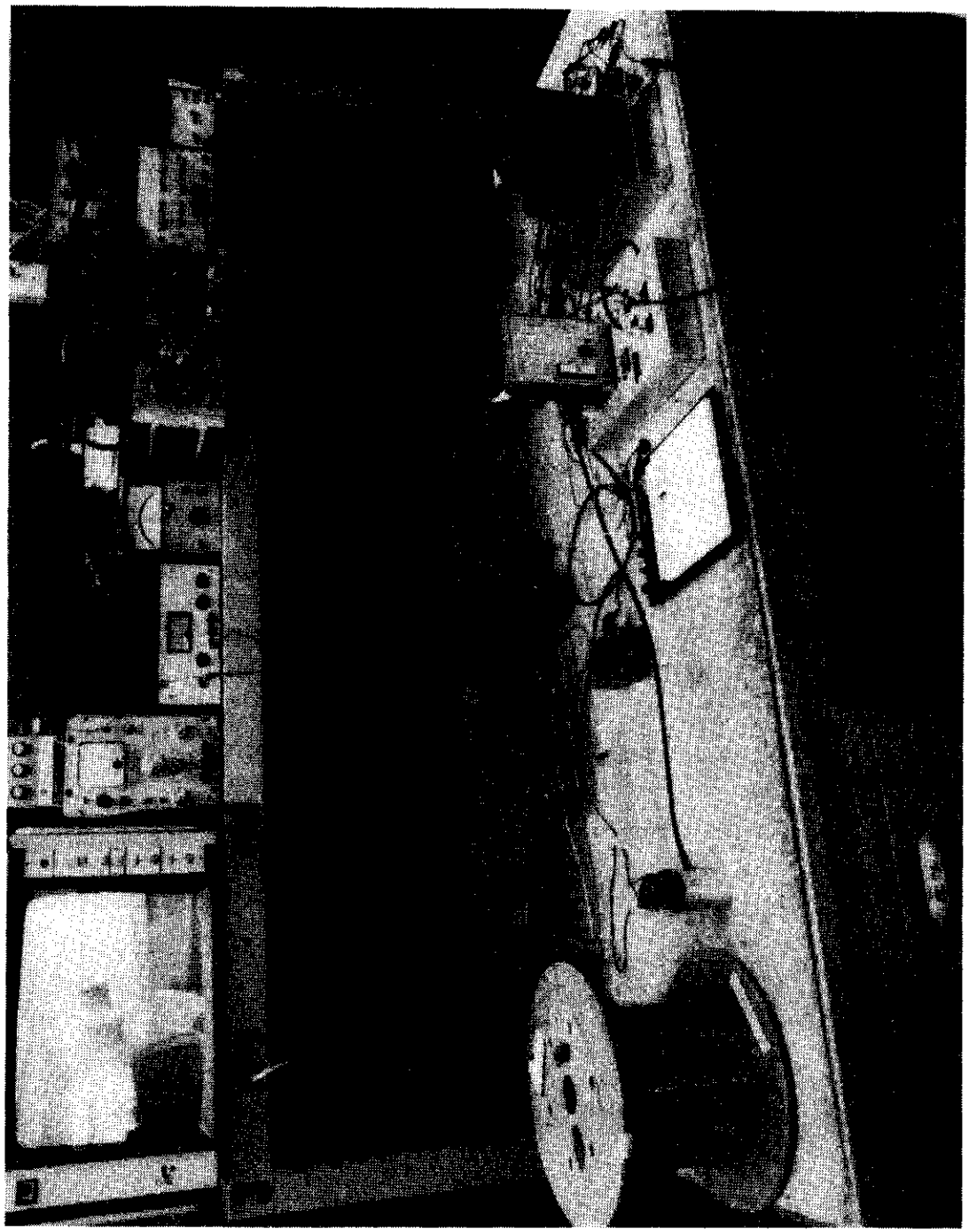

Figure 13. The NOSC prototype brassboard PFM data link.

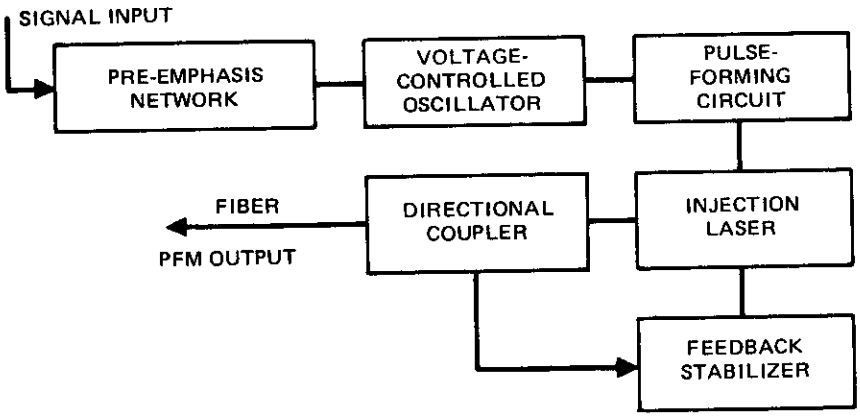


Figure 14. Block diagram of the PFM transmitter used in the NOSC PFM brassboard data link.

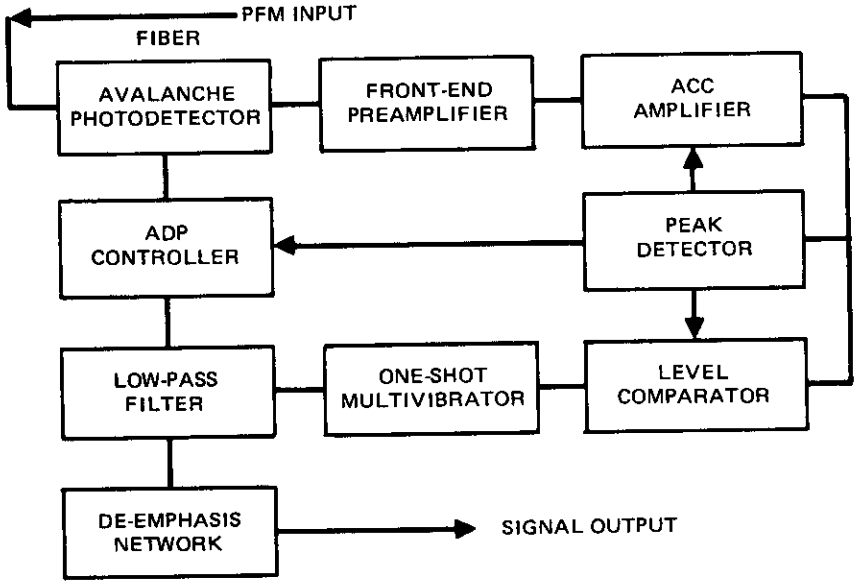


Figure 15. Block diagram of the PFM receiver.

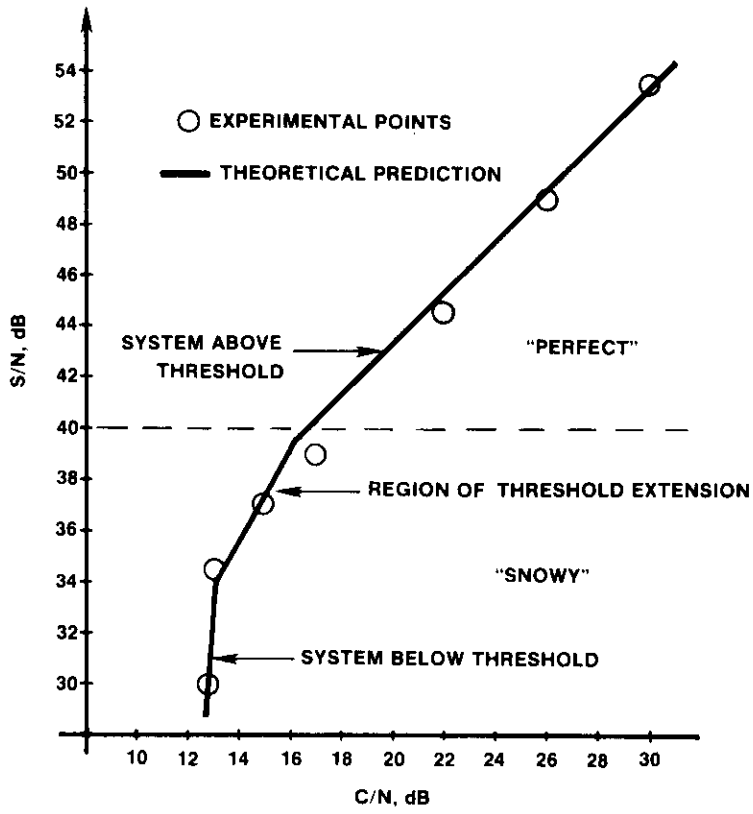


Figure 16. Receiver operating characteristics compared with theoretical predictions.

required to implement optical links on a variety of undersea platforms and devices. The penetrator provides the means by which the optical signals carried by the fiber are transferred between the high-hydrostatic-pressure environment of the cable and the low-pressure environment of the electronics package or manned portion of any underwater system. Thus it is a key component required in practically all proposed underwater fiber-optic applications.

An optimum fiber-optic penetrator design would incorporate the many features that have evolved over a long period and are now available in present-day electrical penetrators. Unless these proven features are fully utilized, undesirable effects could negate the advantages that fiber-optic cables have in comparison with coaxial cables. The following specific design recommendations should be incorporated.

1. The penetrator design should exhibit low optical throughput attenuation. Insertion-loss characteristics should be comparable to and at least as repeatable as the better optical fiber connectors presently available in the marketplace. The optical characteristics should be maintained over the entire spectral region used for communications.
2. The penetrator design should lend itself to efficient certification procedures. It should be possible to test and certify the pressure-integrity function of the

device at the time of manufacture, prior to integration with the cable and optoelectronics. Ideally, the pressure-barrier subcomponent should be standardized and type-certified, and should lend itself to integration with any type of optical fiber or connector when incorporated into its final penetrator configuration.

3. The design should be fully demountable from both the high- and low-pressure sides of the penetrator unit. Ideally, the high-pressure side should be capable of underwater make/break operation, a valuable asset for some important system applications. Full demountability obviates the requirement for treating the penetrator, the optoelectronics assembly, and the cable as a single unit, and allows separation for the purpose of repair, exchange, transport, and storage of the individual subsystems over the life and mission profile of the system.
4. The design should be compatible with a wide variety of optical fiber and connector types. This reduces the certification burden, and also minimizes inventory requirements; one penetrator type should be capable of operation with a wide variety of optical fiber styles by means of a standardized, type-accepted connector body.
5. The design should be straightforward to manufacture in a repeatable fashion with reasonable manufacturing tolerances. It should not be so complex that reliability and cost-effectiveness are compromised.
6. The design should be rugged and robust, which would permit operation over a wide range of temperature and pressure conditions, and should be resistant to damage by vibration and explosive shock. Overall system performance must not be compromised in any way by limitations of the fiber-optic penetrator. In the case of the NOSC free swimmer, the penetrator must be capable of an operating pressure of 1000 psi over a temperature range of 0°C to 40°C.
7. The design should lend itself to hermetic sealing for applications which require sustained exposure to high hydrostatic pressures, and should tolerate no vapor intrusion for reliability reasons. Glass-to-metal or glass-to-ceramic seals should be usable to form a hermetic vapor barrier without requiring a major redesign or recertification effort.

Historically, epoxy-filled hypodermic needles, epoxy pottings, and elastomeric squeeze bushings have been employed when it was required to transfer light from an optical fiber across a pressure gradient. These techniques all realize their light-transfer function by means of physical sealing to the external cable sheath or to the optical fiber itself. Such approaches fail to satisfy all or even most of the criteria that describe a viable penetrator. While these techniques sometimes serve as adequate solutions when applied to the test and evaluation of developmental fiber-optic components, reliance on them would result in undesirable engineering and operational compromises if applied to Navy systems.

The penetrator realization reported here is based on the concept disclosed in ref 14. This approach utilizes a Graded Refractive Index Rod Lens (GRIN) of one-half pitch length as a combination pressure barrier and imaging device (schematically depicted in fig 17).

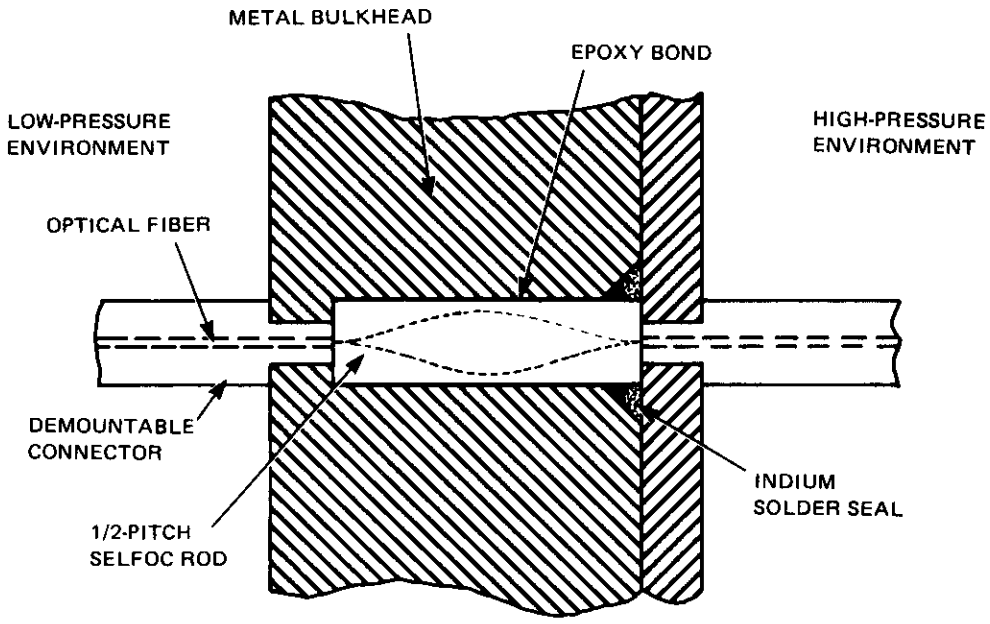


Figure 17. Optical fiber high-pressure penetrator schematic.

A GRIN lens of one-half pitch length has the property of relaying an image, inverted and at unity magnification, from one face to the opposite face. This allows the light from a fiber-optic connector to be imaged onto a conjugate connector with very low insertion loss. The glass rod is sealed into the bulkhead to serve as a pressure window as well as perform the relay lens function (ref 15).

As a result of a development program carried out at NOSC in FY 80 under Internal Exploratory Development funding (ref 16), we are confident that practical, high-performance fiber-optic pressure penetrators are entirely realizable, and that practical production devices are possible to manufacture if suitable fabrication techniques are employed. Prototype demountable penetrator units developed at NOSC, which use the one-half pitch GRIN lens window concept combined with refinements related to positional rod location and connector transverse alignment, exhibit approximately 1–1.5 dB optical insertion loss, which makes them optically comparable to many of the better fiber-optic connectors themselves. Intrinsic insertion loss of the GRIN lens is on the order of 0.4–0.5 dB, which would permit a very low level of insertion loss to be realized in nondemountable designs as well. Units have been tested to hydrostatic pressures in excess of 10 000 psi (corresponding to maximum depths of more than 95% of the ocean floor) without failure. No degradation in optical performance was observed after high-pressure "soaks" lasting several days, which indicates that inconsequential positional creep in rod position was taking place as the result of long-term applied stress. Temperature cycling over a range from –40°C to +100°C caused no glass spalling as a result of mismatch of temperature coefficients between glass and metal. A prototype fiber-optic penetrator is shown in figures 18 and 19.

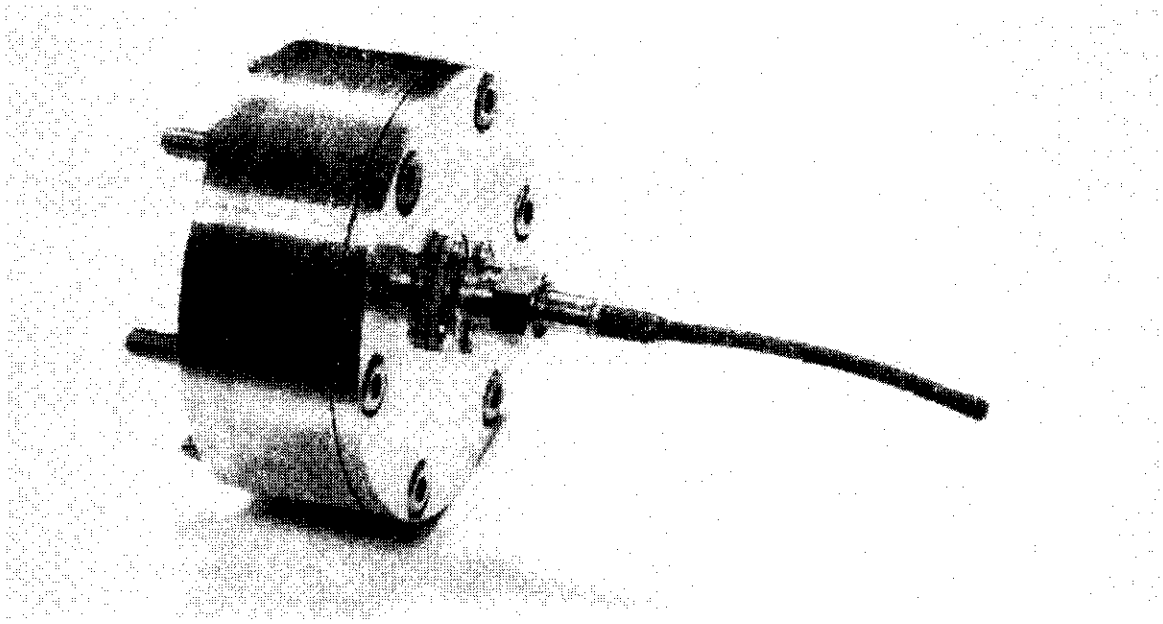

Figure 18. Prototype fiber-optic penetrator (side view).

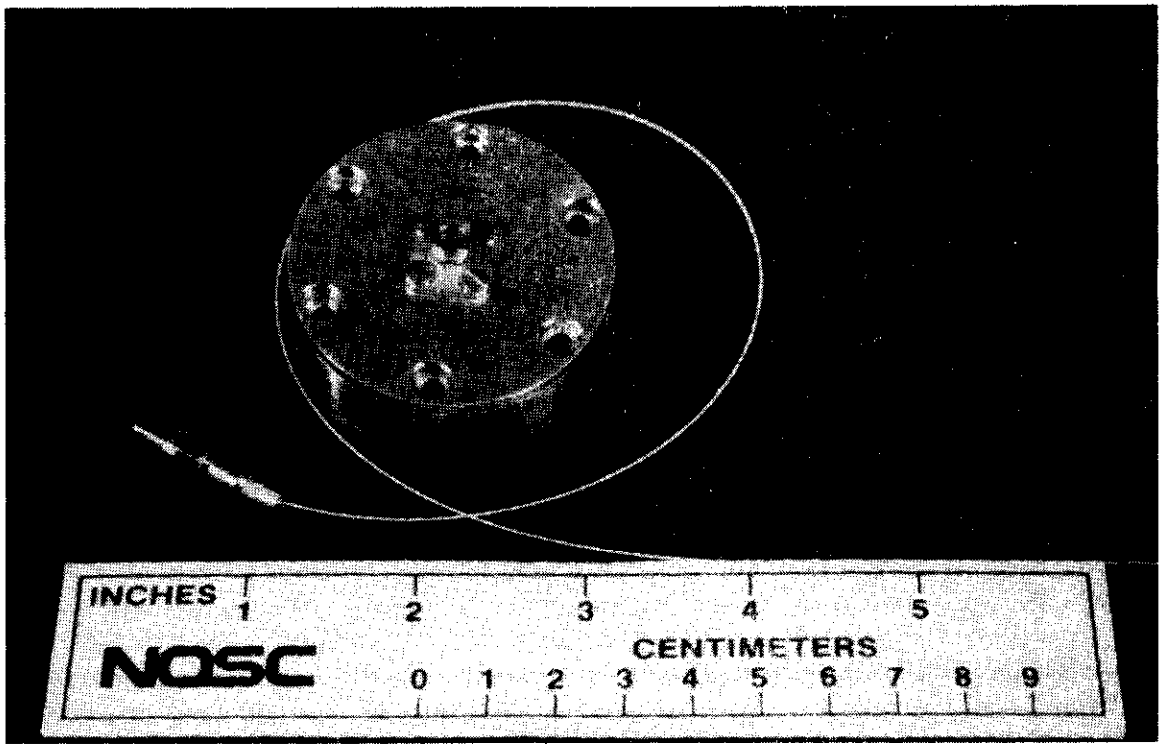


Figure 19. Prototype fiber-optic penetrator (top view).

Such a device, installed on the bulkhead of the communications bottle of the NOSC free swimmer, transfers optical information conveyed by the deployable fiber-optic tether cable to and from the optoelectronics in the vehicle in a robust and reliable manner. The connector on the cable can be demounted in a matter of seconds, allowing rapid replacement of the tether cable spools. This is a valuable feature for practical, at-sea operation of the system. In the event of cable breakage or operator error in installing the connector into the penetrator, there is no danger of water leakage because the penetrator itself provides the pressure integrity function.

## 4.0 CONCLUSIONS AND RECOMMENDATIONS

### 4.1 PROGRESS TO DATE

A fiber-optics communication link for EAVE WEST has been demonstrated in the following areas:

1. A deployed optical fiber cable was payed out underwater from a hand-wound coil mounted on the EAVE WEST free-swimming submersible in 1979 (ref 4). It was demonstrated that both armored and ruggedized optical fibers could be deployed successfully from a free-swimming submersible with little penalty in speed, performance, or power consumption. The tether cable diameters ranged from 0.020 to 0.036 inch, and included both ruggedized and unstrengthened optical fiber units.
2. With knowledge gained from this test of hand-wound fiber canisters, computer-controlled machinery has been constructed for the automatic precision fabrication of long, pretwisted deployment spools at low cost. We are now capable of producing high-capacity, precision-wound spools of expendable optical tether cable in packages suitable for deployment from small undersea vehicles with negligible drag penalty. To date, cable lengths as great as 4 km have been payed out underwater at speeds up to 100 fps.
3. Undersea vehicles need considerable standoff range if they are to be practical for pipeline inspection applications (see appendix). Work was performed in 1978 to demonstrate an optimized fiber-optic coding system, PFM, which allows the ultimate in standoff range to be obtained with any optical fiber transmission line (ref 6 and 7). For use in conjunction with the sync-interleaved data multiplexer, an optimum television/command control data interface has been designed, fabricated, tested, and demonstrated in the laboratory.
4. We are presently experimenting with cabling techniques to ruggedize two ultra-low attenuation optical fibers, each more than 5 km in length, from Sumitomo of Japan. Using fibers of this quality (0.68 dB/km) in conjunction with the PFM electronics operating at 1.57 $\mu$m wavelength, a 25–50-nmi repeaterless standoff range might be obtained.
5. Work has been progressing on a number of ancillary fiber-optic components for use in the ocean. A most important device is the high-pressure penetrator. It would be quite difficult to build a practical undersea system without such a device. We have operated our devices to pressures well in excess of 10 000 psi with no failures, and have surpassed the MIL temperature range of –40°C to +80°C. These devices permit both at-sea demounting of the optical cable from

either side of the bulkhead and underwater connect/disconnect. Our designs are readily configured for hermetic applications.

6. Demonstration of the operation of the EAVE WEST submersible with a supervisory-controlled architecture that incorporates appropriate automatic contingency procedures has been completed (ref 4). This vehicle has been tested in water and has followed a simulated pipeline. Real-time TV has been used to control its movement by means of controls on the vehicle console. A twisted-pair wire link was substituted for the communication link to permit these tests to be conducted early in the development phase.

## 4.2 RECOMMENDATIONS

Since the approach has been determined to be feasible for pipeline and structures inspection, it is recommended that the entire hardware concept be implemented aboard the EAVE WEST submersible and tested in the ocean. Adequate contingency procedures in the event of communication link failure should be implemented in the vehicle control software and also demonstrated during an actual inspection operation.

The major remaining task is the system integration of each of the above technological subareas, and the demonstration of the total system in the water. This is expected to take place early in FY 81. More effort is required in the development of color multiplexing components (ie, wavelength duplexers and optoelectronic components such as transmitters and receivers designed to operate at a variety of wavelengths).

## APPENDIX:

## DEPLOYED CABLE DYNAMICS AND COST FACTORS

A cable dynamics model and computer program were developed at NOSC and used as the bases for the deployment model of a fiber-optics cable. The original program was developed to calculate the nonequilibrium movement of a towed cable with a payload. A tow ship or powered clump moves horizontally at a constant speed, pulling cable and payload behind. The user specifies the initial configuration of a fully deployed cable. The model is two-dimensional, showing movements vertically and horizontally in the X, Y plane. X and Y thrusts are specified for the payload, and there is the capability of varying the thrust at set intervals. The varying payload thrusts, along with tow speed, cable drag, cable weight, and payload drag, are used to determine the cable configurations as a function of time. The tensions at the top and bottom of the cable are also calculated.

The main modification to the original program provides for cable deployment, since the original program models a fully deployed cable with a fixed length. In the deployment model, which features an expendable tether case, cable is paid out continually to form ever-increasing scopes. To begin the deployment program, the user inputs the characteristics of the tether and payload (tethered vehicle). The cable is modeled by straight-line segments. The initial cable configuration is calculated from the number of straight-line segments, the length of these segments, and the locations of the nodes at the end points of the segments. After the initial length is specified, the total amount of tether in the payout reel available for deployment is specified. The user specifies the intervals at which the computer is to print out the catenary configuration, and how often.

To start the deployment, the tow ship starts forward at a fixed speed. The capability of simulating a ship with automatic stationkeeping can be achieved if the coordinate system is translated to have the origin move with the top of the cable. In this case, the tow speed becomes the uniform current speed that is moving past the stationary ship. The simulation either starts with a tow ship moving at a fixed speed with no current, or with a ship on automatic stationkeeping with a constant, uniform current.

The submersible starts on a course whose speed and heading are specified by the user. The program calculates the location of the underwater vehicle and deploys new lengths of tether to keep up with the moving vehicle. At the same time, the cable configuration and tensions are calculated for the deploying cable in response to ship movement, vehicle movement, and current. The program keeps track of how much tether is deployed and continues even after full deployment.

The payout of cable is assumed to take place only from a canister on the tethered vehicle. A pullout tension of zero is assumed. Thus the tethered vehicle cannot provide any pull on the cable during deployment. Any movement or thrust from the tethered vehicle merely pays out more tether. This approximates the unarmored f-o tether well, but there will probably be a substantial pullout tension for the S-glass tether. Because of this, the program actually gives a "worst-case" condition. The reason is that a nonzero tension will result in less cable being pulled out by the current.

The program starts with an initial cable configuration and either a current or tow ship speed, as well as a tethered vehicle speed. The current (or tow ship) movement and the movement of the tethered vehicle will pay out tether until all available cable is deployed. The program continuously calculates the cable tensions, configuration, and scope.

The different fiber-optic tether configurations can be simulated with this deployment model for different test conditions. The tensions during and after deployment help to

determine which configuration is most suitable for use as a tether for a particular mission scenario. The cable scope and required standoff will dictate the magnitude of the binding force desired on the payout reel. The available vehicle thrust must then be checked to ensure that it is sufficient to overcome vehicle drag and cable pullout forces.

The cost of Outer Continental Shelf inspection of pipelines and structures is an important consideration. Since the link is meant to be expendable, it is desirable to pay out a minimum length of tether, lest the mission become too costly. The total amount of deployed fiber-optic link is therefore an important parameter. However, there is a minimum length that must be payed out. This is the straight-line distance to the payload. The ratio of the straight-line distance to the total amount of deployed cable is called the effective length ratio (ELR).

It was found that for different vehicle paths and different currents, there was a wide variation in the ELR. In the worst case tested, it was 0.29 and in the best case 1.00. This means that, under some conditions, there could be payed out more than three times as much cable as the straight-line distance, while at other times no such penalty would occur.

The results of testing three vehicle paths will be given here. In the tests, important cable properties as well as current speed were varied. The weight and diameter were varied to simulate the different types of optical fiber tethers under study, and the current was varied to simulate different environmental conditions. The properties of the different tether cables are listed below.

| | Unarmored Optical Fiber | Ruggedized S-Glass | Almost Neutrally Buoyant Fiber |
|---|---|---|---|
| OD, inches | 0.018 | 0.027 | 0.027 |
| Weight per Unit Length in Water, lb/ft | $3.27 \times 10^{-5}$ | $1.75 \times 10^{-4}$ | $1.00 \times 10^{-7}$ (in seawater) |
| Present cost | \$0.25 – 2.50 | \$0.75 – 1.75 | Unavailable |

In all the mission trajectories presented in this report, the vehicle ends up approximately 1077 feet from the mother ship. This is accomplished by diving for 10 minutes at 0.25 knot and moving horizontally at 1 knot for 10 minutes. On the first three graphs that follow, the vehicle dives first and then heads into the current. The next three have the vehicle diving and then heading with the current. In the final three graphs, the vehicle first heads into the current and then dives. In these graphs, the current ranged from 0.1 knot to 0.5 knot and was varied in steps of 0.1 knot.

It was found that very few generalizations could be made about which paths and which cables proved superior. Most of the time, better ELRs were noted for weaker currents (as might be expected), but this was not always the case. Heavier cables tended to be inferior to light cables in weak currents (0.1 or 0.2 knot), but they would be superior in strong currents (0.4 or 0.5 knot). The reason is that it is harder to push heavier cables out into their catenary-like shape. Stronger cables might tend to permit higher deployment tensions, thus inhibiting catenary formation. Neutrally buoyant designs do not appear desirable in either case. One important general result is that substantial benefits can be enjoyed if the vehicle travels with the current, instead of into it (a novel mode in the case of conventional tethered vehicles). For example, in the case of a vehicle deploying an S-glass-type tether heading into a 0.5-knot

current, after 20 minutes it has an ELR of 0.39; but heading in the same direction as the current, an ELR of 0.85 is given. This represents a savings of 54% in the amount of tether deployed.

Work is currently in progress to achieve at-sea deployment tests of up to 1 km of tether; the computer model will provide the preliminary analysis for defining the pullout force in the intended test scenario. The deployment spools will be fabricated by means of the automated, microprocessor-controlled winding machine, and data will be generated and documented on the binding agents used and the winding procedures developed.

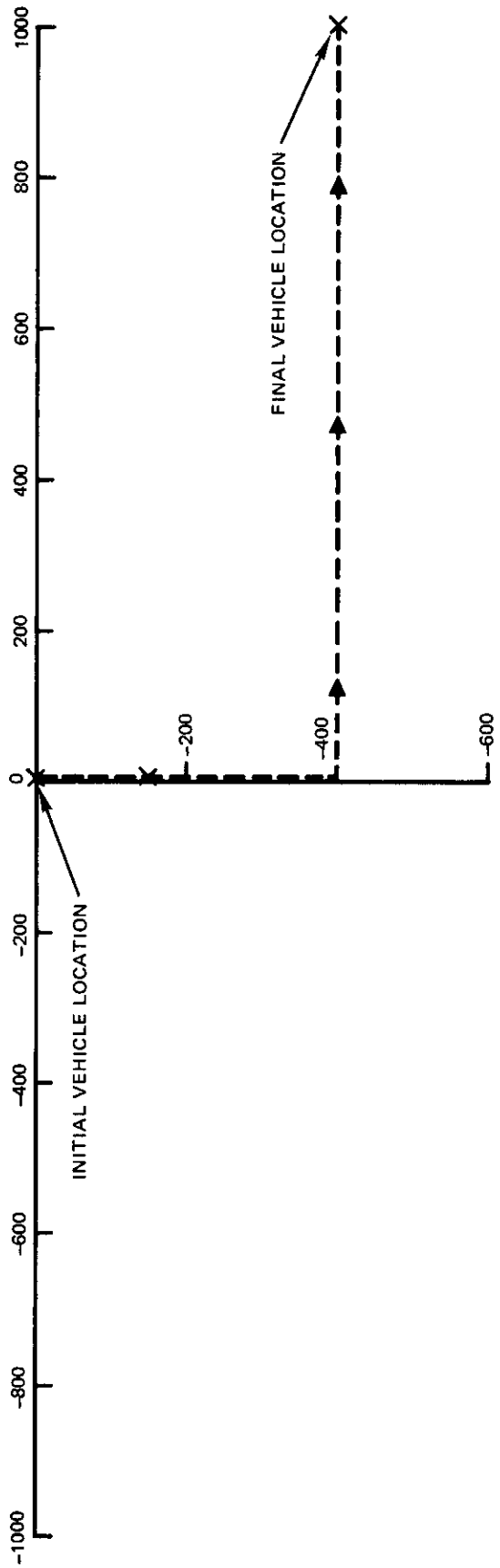


Vehicle path 1.

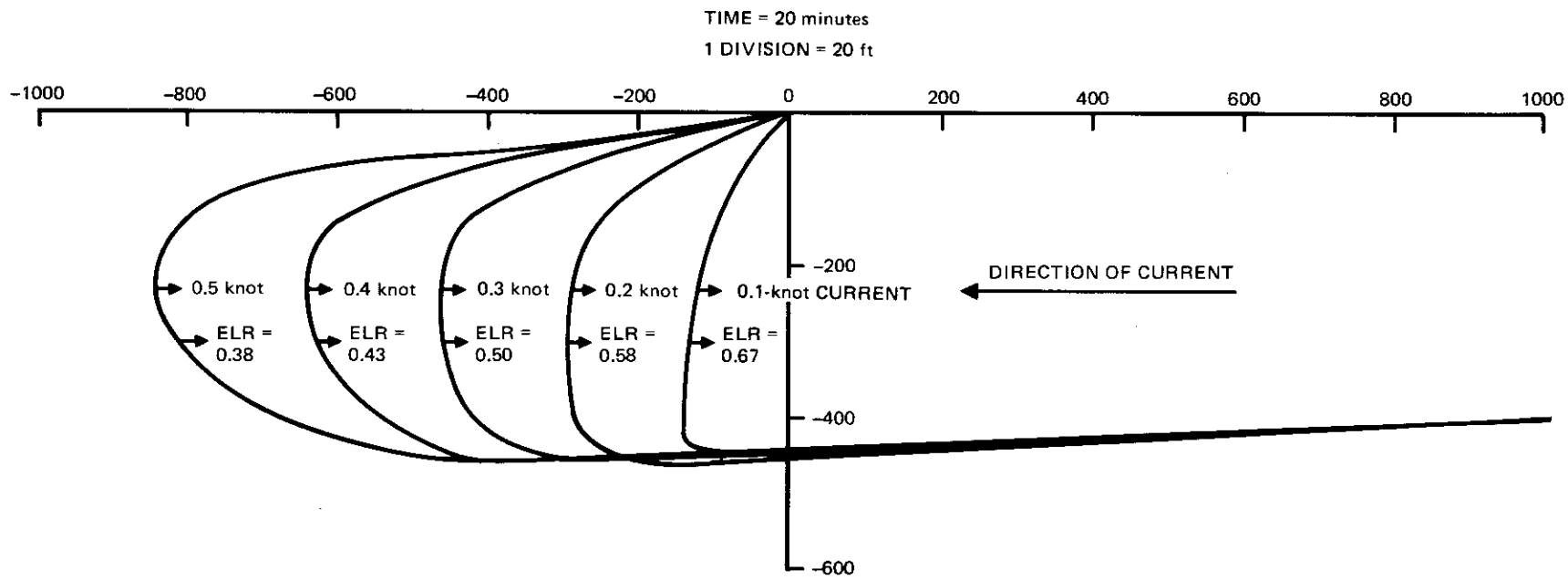


Vehicle with unarmored f-o tether heading into current after diving.

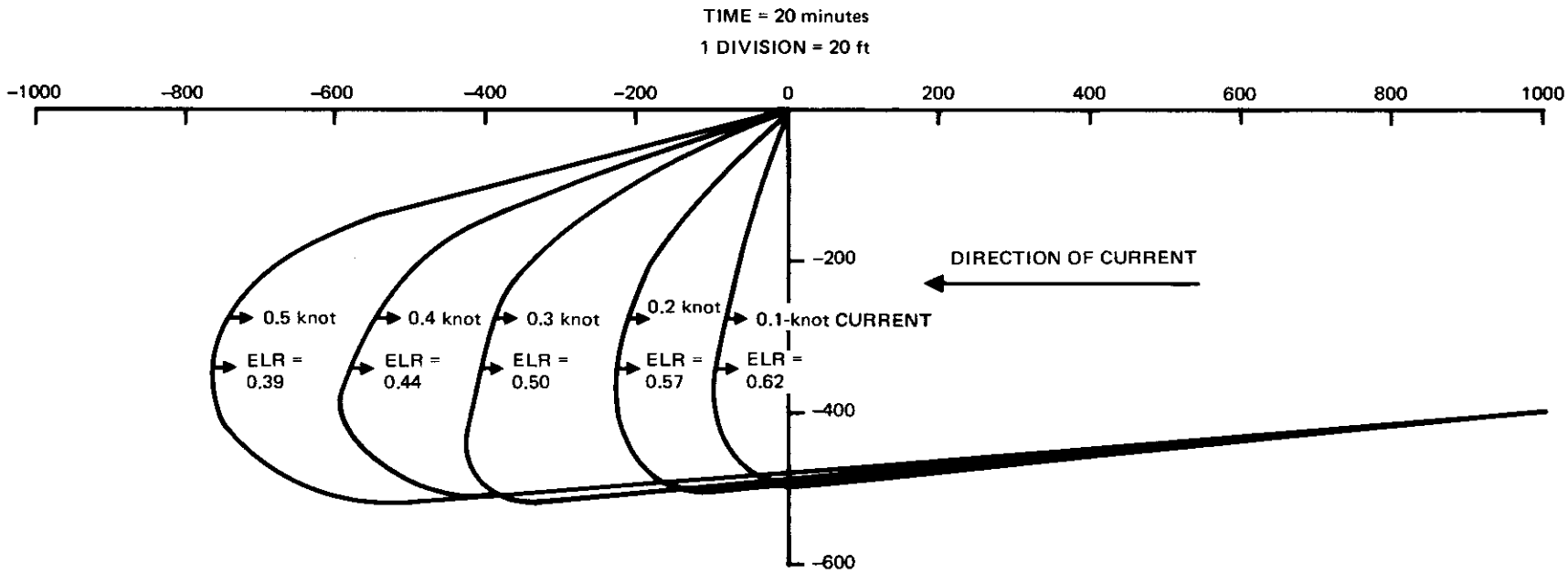


Vehicle with S-glass cable heading into current after diving.

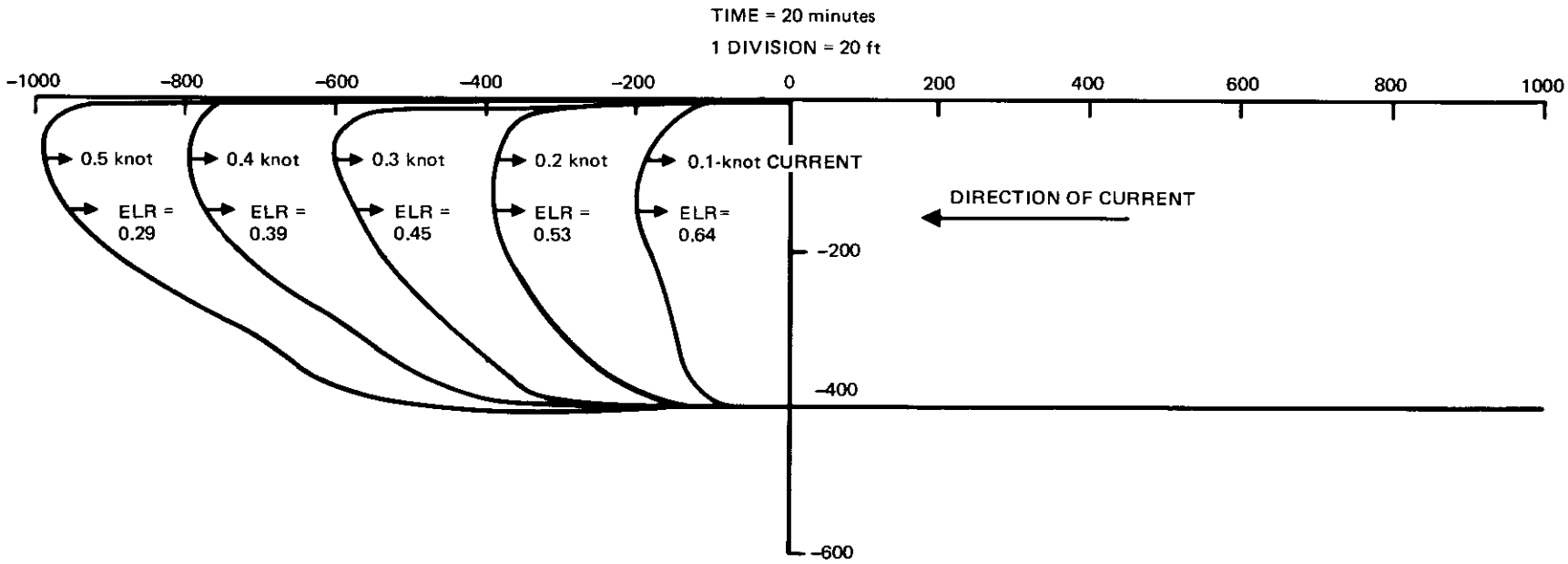


Vehicle with almost neutrally buoyant cable heading into current and then diving.

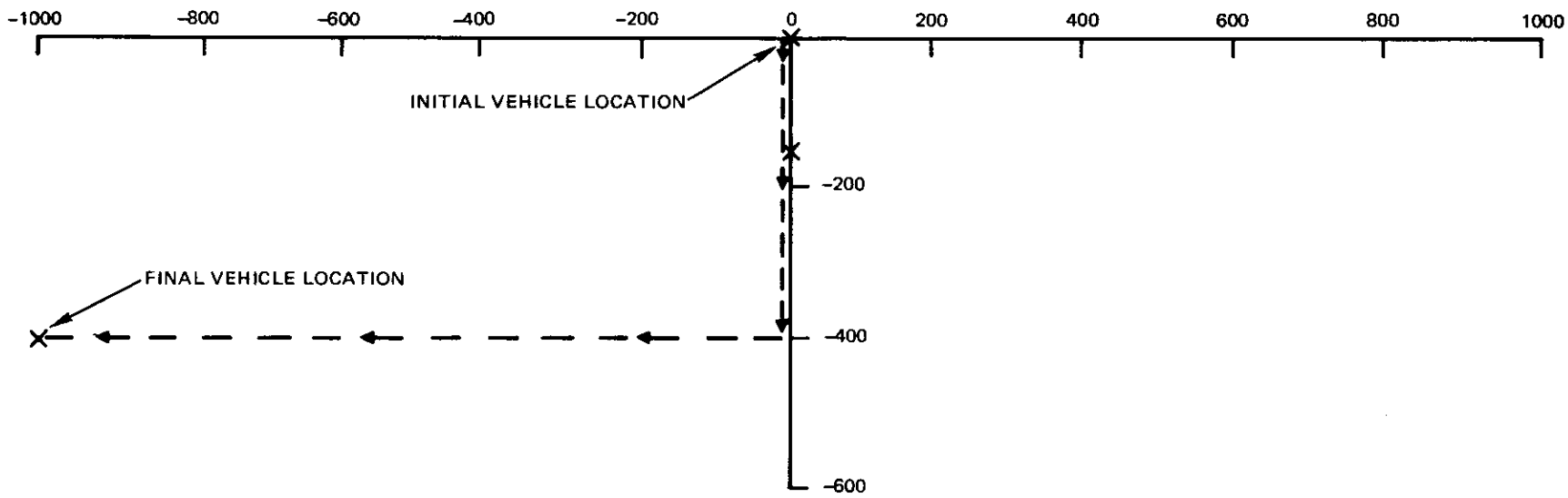


Vehicle path 2.

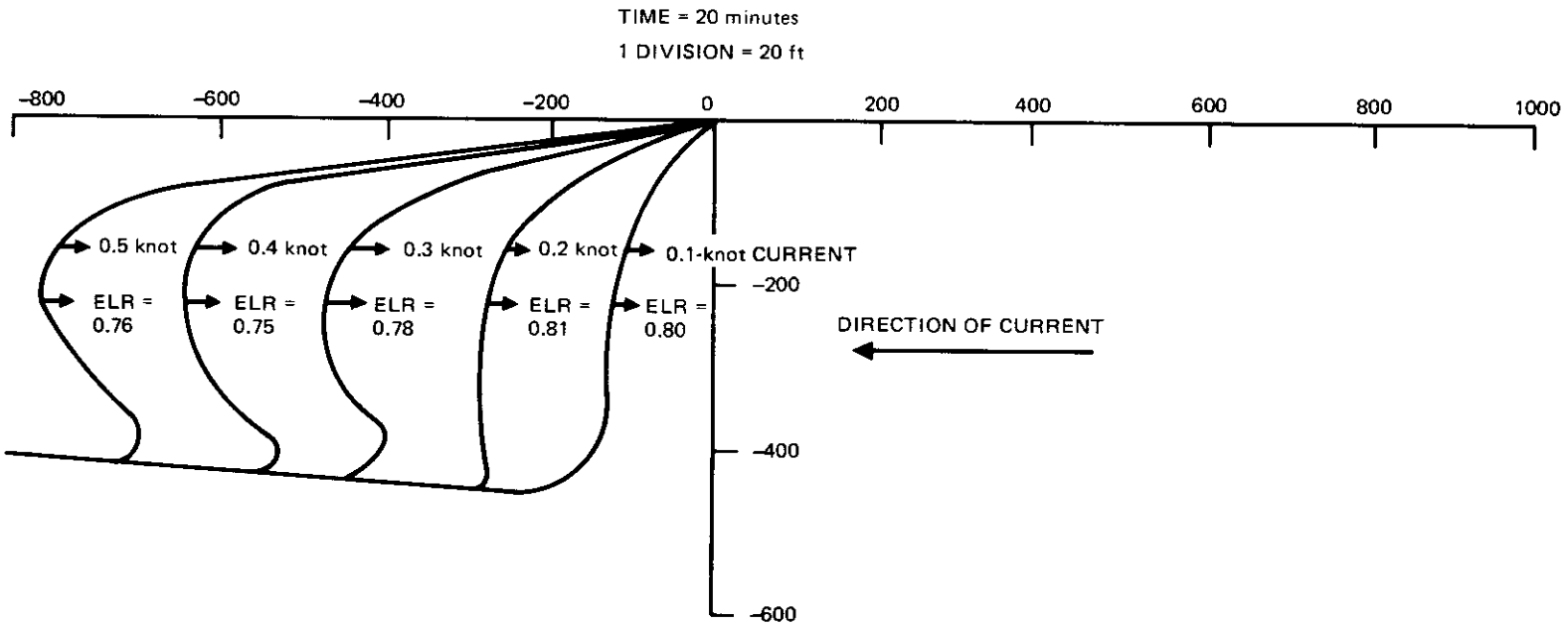


Vehicle with unarmored f-o tether heading with current.

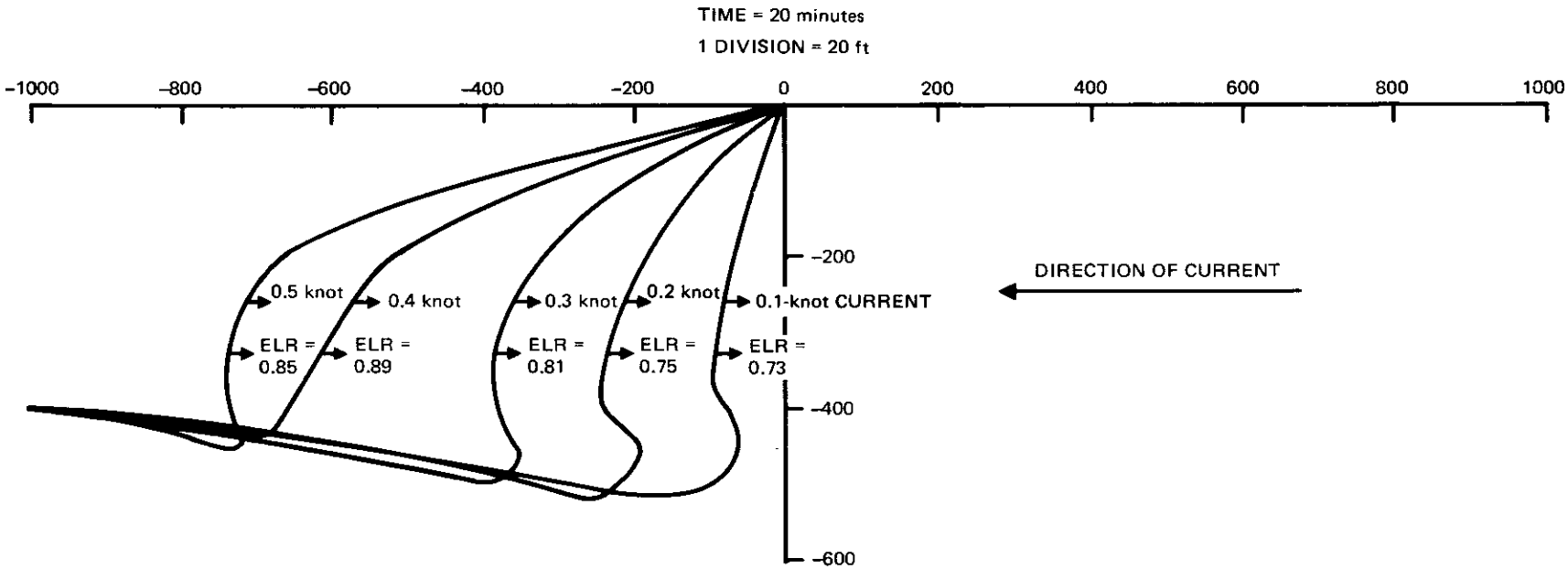


Vehicle with S-glass tether going with the current.

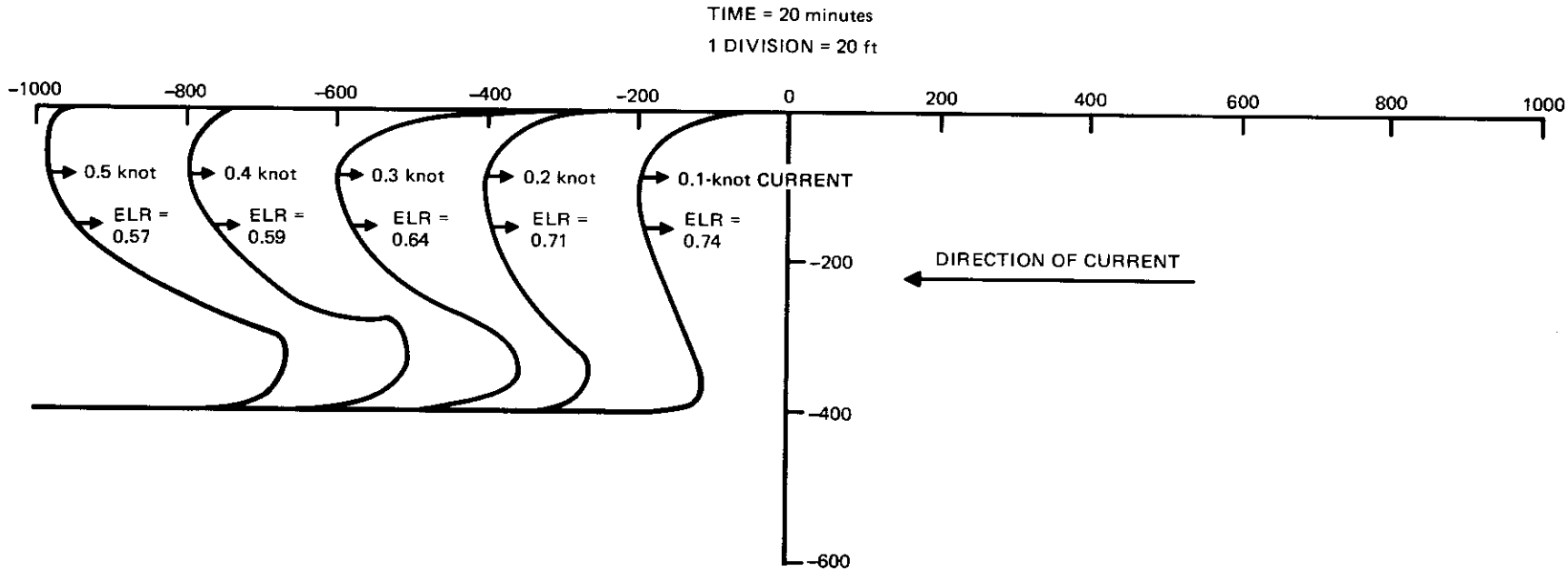


Vehicle with almost neutrally buoyant cable heading with current.

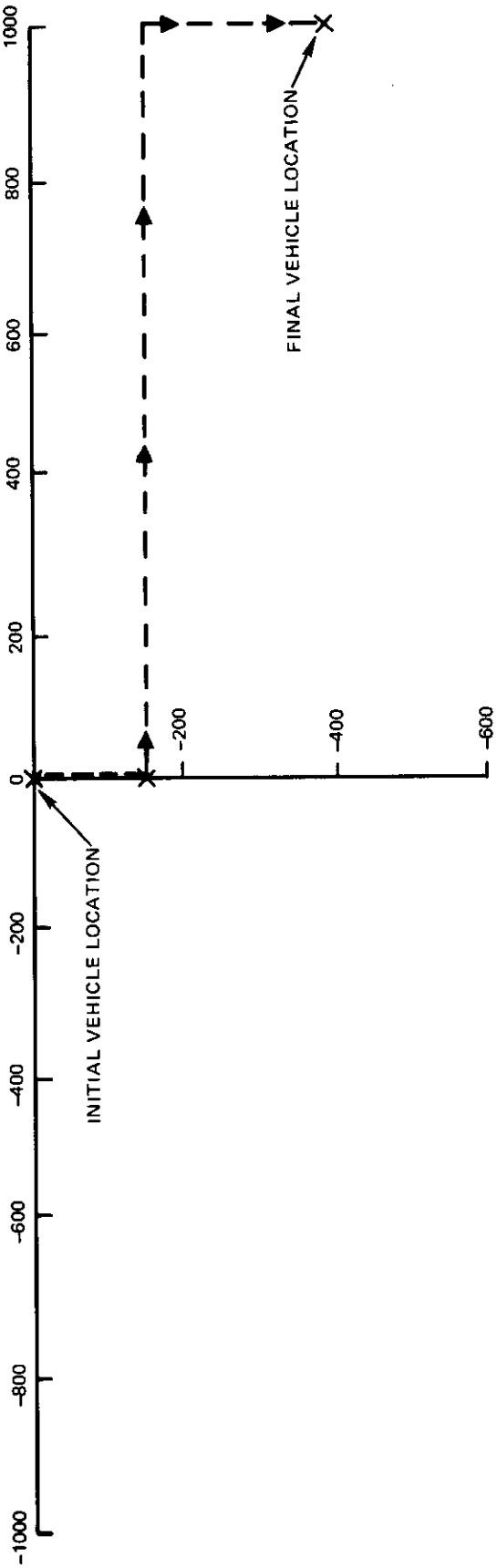


Vehicle path 3.

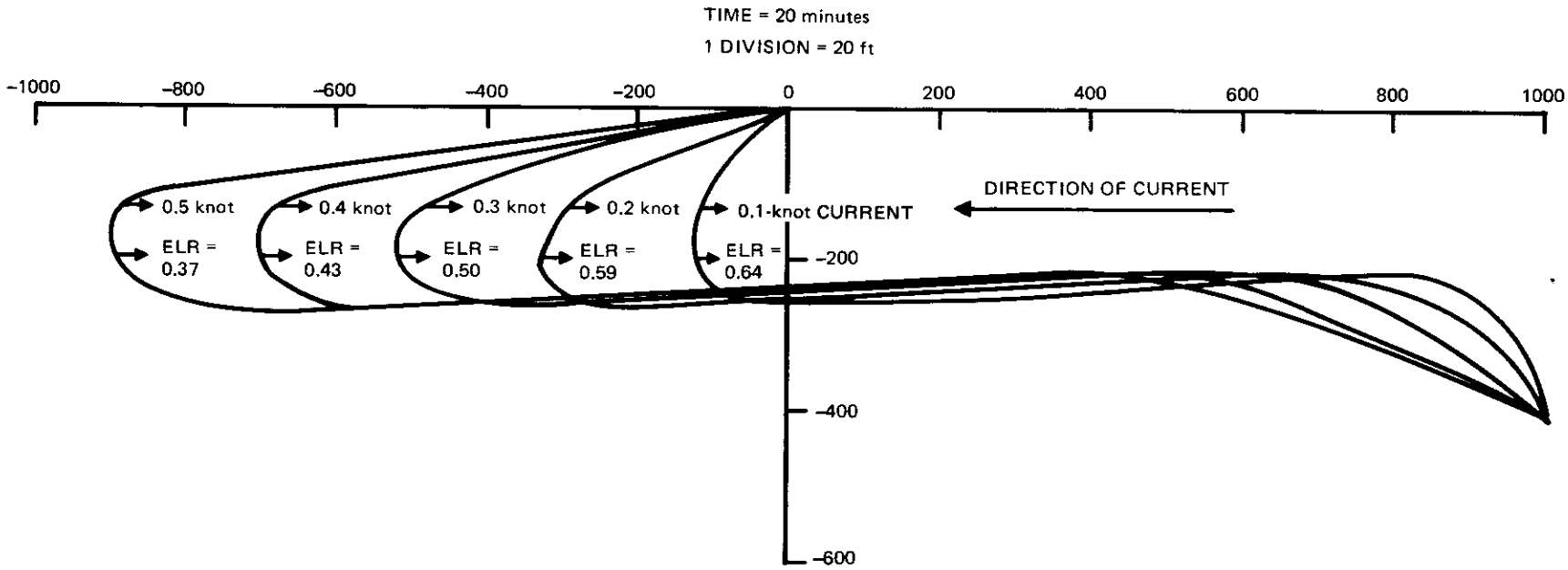


Vehicle with unarmored f-o tether heading into current and then diving.

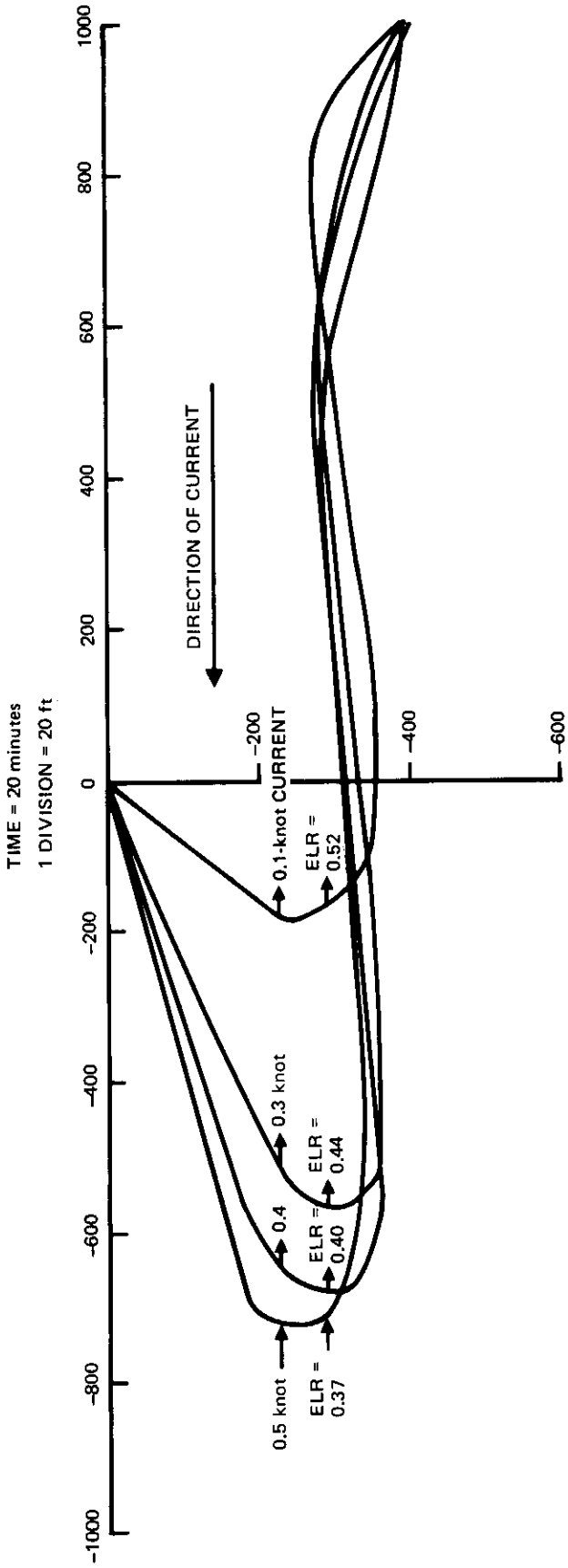


Vehicle with S-glass tether heading into current and then diving.

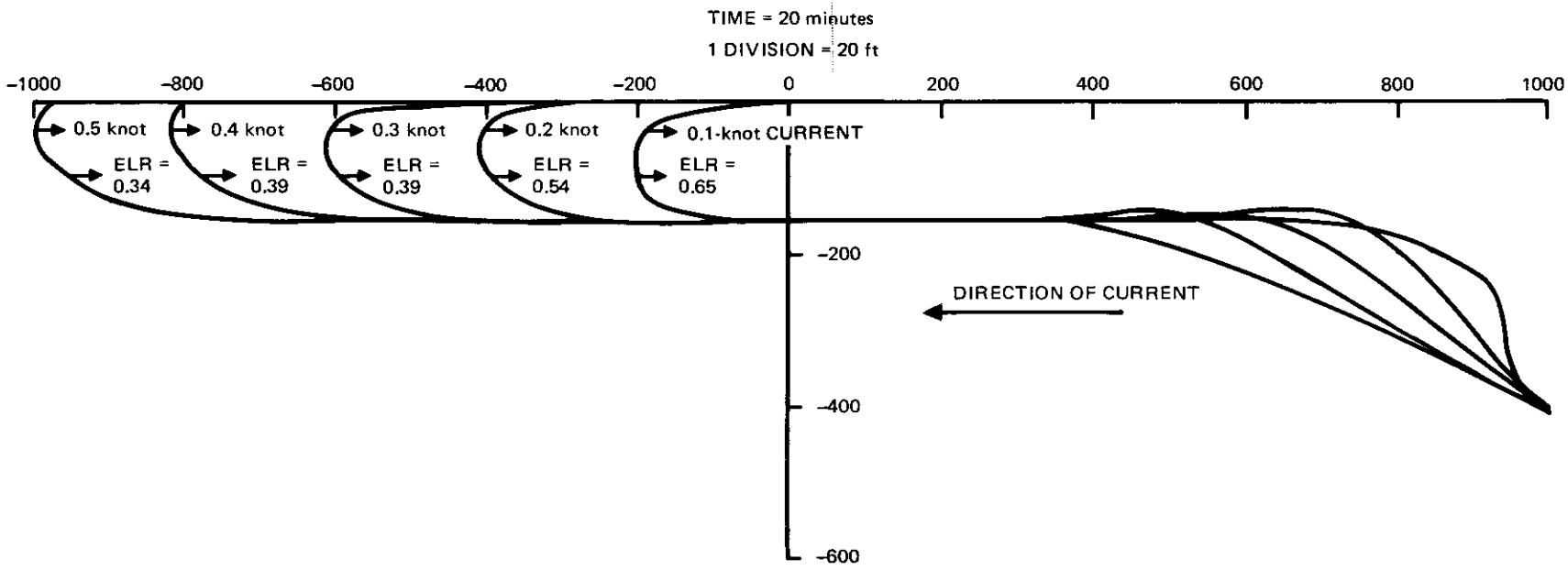


Vehicle with almost neutrally buoyant tether heading into current after diving.

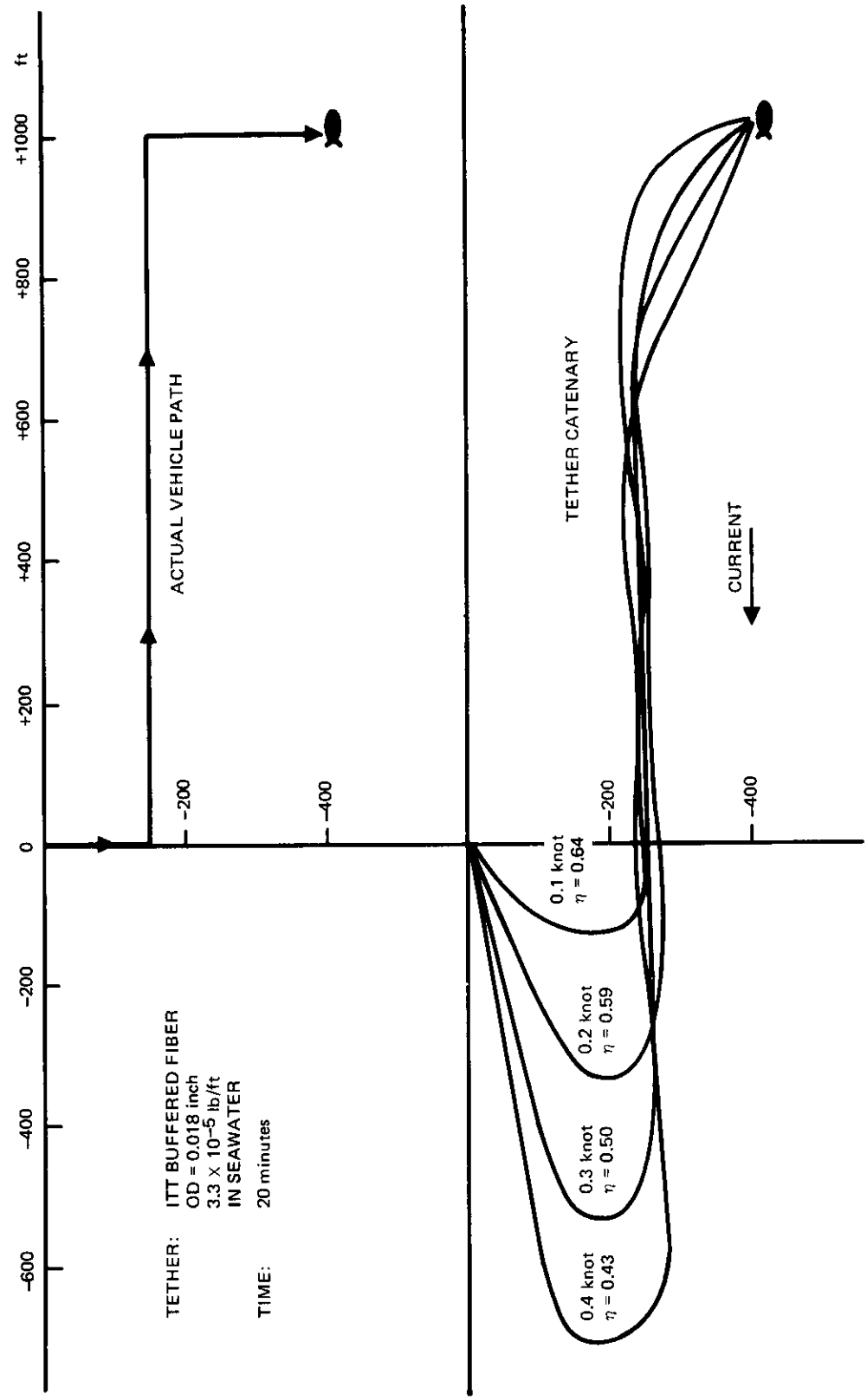
ft
+1000
+800
+600
+400
+200
0
-200
-400
-600
ACTUAL VEHICLE PATH
-200
-400
TETHER CATENARY
CURRENT
-200
-400
0.1 knot
η = 0.64
0.2 knot
η = 0.59
0.3 knot
η = 0.50
0.4 knot
η = 0.43
TETHER: ITT BUFFERED FIBER
OD = 0.018 inch
3.3 X 10⁻⁵ lb/ft
IN SEAWATER
TIME: 20 minutes

## REFERENCES


1. R. Frank Busby Associates, Underwater Inspection/Testing/Monitoring of Offshore Structures, February 1979 (Commerce Contract 7-35336).

2. NOSC TR 217, FY 77 Subsea Solar Scan Acoustic Television (SUBSAT) Tests, by A. Gordon, March 1978.

3. Experimental Autonomous Vehicle Program EAVE; Development of Unmanned, Untethered Submersible Technology for Inspection Tasks, prepared for USGS Research and Development Program for Outer Continental Shelf Oil and Gas Operations.

4. Heckman, P. J., and H. B. McCracken, An Untethered, Unmanned Submersible, Proceedings of Oceans '79, September 1979, p 733–737.

5. NOSC TR 622, Free-Swimming Submersible Testbed (EAVE WEST), by Paul J. Heckman, September 1980.

6. Gloge, D., Bending Loss in Multimode Fibers with Graded and Ungraded Core Index, Applied Optics, v II, 1972, p 2506–2513.

7. NOSC TR 632, Development of an Underwater Manipulator for Use on a Free-Swimming Unmanned Submersible, by Peter Bosse and P. J. Heckman, October 1980.

8. Timmerman, C. C., Signal-to-Noise Ratio of a Video Signal Transmitted by a Fiber Optic System using Pulse Frequency Modulation, IEEE Transactions on Broadcasting, v BC-23, no 1, March 1977.

9. Cowen, S. J., Fiber Optic System for Transmission of Video Signals by Pulse Frequency Modulation, Proceedings of Oceans '79, September 1979, p 253–259.

10. Cowen, S. J., Fiber Optic System of Video Signals by Pulse Frequency Modulation, patent application under U.S. Navy case no 63094, 15 February 1980; disclosed 9 April 1977.

11. Tobey, G. E., J. G. Graeme, and L. P. Huelsman, Operational Amplifiers; Design and Applications, McGraw-Hill, 1971, p 419–420.

12. Pauter, P. F., Modulation, Noise and Spectral Analysis, McGraw-Hill, 1965, p 506, 536.

13. Cowen, S. J., G. Wilkins, and C. Chang, Fiber Optic Duplex Dichroic Coupler, NOSC patent disclosure, June 1979.

14. Redfern, J., High Pressure Optical Bulkhead Penetrator, U.S. Patent 3,825,320, filed 2 March 1973; granted 23 July 1974.

15. Cowen, S. J., J. H. Daughtry, C. Young, and J. Redfern, Undersea High Pressure Bulkhead Penetrator for use with Fiber Optic Cables, U.S. Patent, Navy case no NOSC-86, filed November 1980.

16. NOSC TR 644, A High-Performance Optical Fiber Pressure Penetrator for use in the Deep Ocean, by S. J. Cowen, in preparation.